JOHANNES KEPLER
UNIVERSITÄT LINZ
Netzwerk für Forschung, Lehre und Praxis

Studies towards a bio – organic – cell – chip interface

DIPLOMARBEIT

zur Erlangung des akademischen Grades

DIPLOMINGENIEUR

in der Studienrichtung

WIRTSCHAFTSINGENIEURWESEN FÜR CHEMIE

Angefertigt am *Linz Institute for Organic Solar Cells (LIOS)*

Betreuung:

o. Univ.-Prof. Dr. Serdar N. Sariciftci

Eingereicht von:

Andreas Spiegel

Linz, Oktober 2006

Eidesstattliche Erklärung:

Ich erkläre an Eides statt, dass ich die vorliegende Diplomarbeit selbstständig und ohne fremde Hilfe verfasst, andere als die angegebenen Quellen und Hilfsmittel nicht benutzt bzw. die wörtlich oder sinngemäß entnommenen Stellen als solche kenntlich gemacht habe.

Linz, im Oktober 2006

Andreas Spiegel

Abstract

In the course of this work preliminary experiments towards the feasibility of junctions between cells and electronic devices were performed.
First of all the compatibility of human embryonic kidney (HEK) cells towards a broad range of untreated organic insulators and organic semiconductor materials was tested.
Based on these results calcium channels were expressed in HEK cells and those should be stimulated capacitively which didn't work because the Ca^{2+} channel couldn't be expressed thoroughly in the HEK293 cell culture.
We also looked for a correlation between the adherence of cells to the surface of the dielectric and the Impedance and Capacitance, respectively.
With the materials which were compatible to the HEK cells we fabricated top gate transistors, because these seem to be predestined for the role of electronic devices in a cell chip junction.

Zusammenfassung

Im Rahmen dieser Arbeit wurden Voruntersuchungen zur Machbarkeit von Verbindungen zwischen Zellen und elektronischen Baugruppen wie etwa Transistoren durchgeführt.
Zu diesem Zweck wurde als erster Schritt die Verträglichkeit diverser unbehandelter organischer Isolatoren und organischer Halbleitermaterialien für Human Embryonic Kidney (HEK) Zellen getestet.
Aufbauend auf diese Ergebnisse wurde versucht Kalzium - Ionenkanäle von den HEK – Zellen ausbilden zu lassen und diese dann mittels kapazitiver Stimulation anzuregen, was daran scheiterte, dass die Ausbildung der Kanäle nicht ausreichend möglich war.
Des Weiteren wurde nach Zusammenhängen zwischen Impedanz bzw. Kapazität und anhaften von Zellen an der Oberfläche des Isolators gesucht.
Mit den aus den Verträglichkeitsuntersuchungen hervorgegangenen Materialien sollten außerdem Top – Gate Transistoren gebaut werden, da diese als elektronische Baugruppe für eine Verbindung mit Zellen prädestiniert sind.

Acknowledgement

The presented work was carried out at the Linz Institute for Organic Solar Cells (LIOS), Physical Chemistry, Johannes Kepler University Linz, between October 2005 and October 2006.
I want to thank o. Univ. Prof. Dr. Serdar N. Sariciftci for this very interesting topic, guidance and advice in the last year.

I also like to thank Dr. Birendra Th. Singh for great advice and support.

I thank all present and (former) members of our Institute: Dr. Helmut Neugebauer, (Dr. Gilles, Dennler), (Dr. Farideh Meghdadi), (Dr. Nenad Marjanović), DI Roppert Koeppe, DI Christoph Lungenschmied, DI Anita Fuchsbauer, (Dr. Le Huong Nguyen), DI Martin Egginger, (Dr. Shengli Lu), (DI Hans-Jürgen Prall), Philipp Stadler and Pinar Senkarabacak, for many fruitful discussions and suggestions, on and off the topic.

Thanks also to our secretaries and technician Petra Neumaier, Birgit Paulik, Erika Bradt, Gerda Kalab and Manfred Lipp, which help through the bureaucratic problems and supported me with technical assistance.

Also I'd like to thank the following members of the Biophysics Institute: Dr. Peter Pohl, Dr. Christoph Romanin, Dr. Klaus Sommer, and especially Sabine Buchegger, who supported me with healthy HEK293 cells.

I want to thank furthermore my colleagues during the last years of our studies: Cornelia Kock, Philipp Stadler, Sabrina Heiml, Bernhard Gallistl and Martin Nausner.

Especially I'd like to thank Sabine for supporting me in the last year in every possible way.

Last but not least I'd like to thank my parents for supporting me during the years of my studies.

Für meine Eltern Ernst und Maria Spiegel,
ohne deren Hilfe dieses Studium nicht möglich gewesen wäre.

Curriculum Vitae

Andreas Spiegel

Personal Data:

Name	Andreas Spiegel
Date / Place of Birth:	09.07.1981 in Vöcklabruck
Nationality	Austrian
Marital status	unmarried
Address	Bernaschekstr. 5, A-4664 Oberweis
Parents	Ernst Spiegel, technical engineer
	Maria Spiegel, physician assistant, registered nurse

Education:

10/2005 – 10/2006	Diploma thesis at the Institute for Physical Chemistry, JKU Linz
10/2000 – 12/2006	Studies at the Johannes Kepler University in Linz
	Economics/Chemical Engineering
09/1991 – 07/1999	Grammar School: RG Lambach
09/1987 – 07/1991	Primary School VS Laakichen Süd

Military Service:

09/1999 – 04/2000	Technical Pioneer Corps (PiB3/Tech) Melk

Qualifications:

Languages	German (mothertonque), English (fluent), French (beginner)
Computer	MS Word, MS Excel, Origin
Driving License	since 1999 (B), since 2001 (gantry crane)

Related Experience:

Tutor for General Inorganic Practicum

Tutor for Advanced Inorganic Practicum

Co-Worker at the Linzer Institute for Organic Solar Cells (LIOS)

Further Employees:

Summer 1997	Building Yard, Laakirchen
Summer 1998 & 2002	Superintendent at the public swimming pool, Laakirchen
May 2000	Bavarian Red Cross
June/July 2000	Internship at HIPP GmbH, Gmunden, as receptionist
August 2000	Internship at MIBA AG, Laakirchen, galvanization plant
Summer 2001	Internship at UPM Kymmene, Steyrermühl, waste water Treatment plant
Summer 2003, 2004, 2005:	Internship at UPM Kymmene, Steyrermühl paper production PM3 & PM4

Interests:

Volleyball, Biking, Soccer, Tennis

Contribution to Conferences:

"Study of Ion-selective and bio-functionalised materials for selective field-effect sensing applications"

A. Spiegel, Th. B. Singh, N.S. Sariciftci, K. Sommer, P. Pohl

E-MRS Spring Meeting, May 2006, Nice (France)

Contents:

1. Motivation 1
2. Introduction 3
2.1. Cell-Chip Junction 3
2.1.1. Point contact model 5
2.1.2. Area contact model 5
2.2. Signaling in Biology 7
2.2.1. The Cell 7
2.2.2. The plasma membrane 8
2.2.3. Membrane transport: 10
2.3. Signaling in Information Technology 16
2.3.1. The (organic) capacitor 16
2.3.2. Working principle of LCR meter 17
2.3.3. Organic Semiconductors 19
2.3.4. The (organic) field-effect transistor 20
2.3.5. Operating principle of OFETs 22
3. Experimental 24
3.1. Compatibility test 24
3.1.1. Sample Preparation 24
3.1.2. Sterilization 24
3.1.3. HEK293 cell line 24
3.1.4. Cell culturing 25
3.1.5. Tested materials 25
3.1.6. Light microscopy 29
3.1.7. Pre-treatment of dielectric surfaces 30
3.2. Activation of ion channels in HEK cells 31
3.2.1. Device Preparation 32
3.2.2. Dielectric check 33
3.2.3. Transfection 33
3.2.4. Imaging 35
3.3. Impedance measurements 36
3.4. Capacitance Measurement 36
3.5. I-V Measurements 37

3.6. Top gate transistor 37
3.6.1. Device preparation 37
4. Results and Discussion: 39
4.1. Results of Compatibility test 39
4.1.1. Dielectrics 39
4.1.2. Semiconductor materials 46
4.2. Activation of ion channels in HEK293 cells 49
4.2.1. Transfection results 49
4.3. Impedance measurements 52
4.4. Capacitance Measurement 53
4.4.1. MIM results 53
4.4.2. Capacitance measurement under cell influence 54
4.5. Top gate transistor 55
5. Conclusions 58
6. References 59
7. List of Figures 62
8. Appendix 65
8.1. Appendix A – Dulbecco's Modified Eagle Medium (GIBCO) 65
8.2. Appendix B: Transfection Protocols 66
8.2.1. Transfection Protocol for Transfectin™ Lipid Reagent by *BIO-RAD* 66
8.2.2. Transfection Protocol for Superfect™ by *Quiagen* 66
8.2.3. Transfection Protocol for ExGEN™ by *Fermentas* 66
8.2.4. Transfection Protocol for Lipofectamin™ by *Invitrogen* 67
8.3. Appendix C: Used equipment 67

1. Motivation

Since the rise of information technology or even earlier it has always been a dream for scientists and science fiction authors to get another interface between computer and user than the typical keyboard-hand and screen-eye connection.

In fact it was Luigi Galvani (1737-1798) who first interfaced biology and electricity by accidentally activating frog muscles when one of his assistants touched an exposed nerve in a dissected frog leg with an electrically charged scalpel which then kicked out [1]. Later his experiments lead the way to electrochemical cells invented by Alessandro Volta.
After nearly 200 years W. Shockley, J. Bardeen and W. Brattain [2, 3] re-invented the transistor (J.E. Lilienfeld patented already devices based on the field effect in the year 1930 [4]) in December 1947 in the Bell Labs and earned the Noble Prize for this invention [5]. This and the invention of the MOSFET (metal oxid semiconductor field-effect transistor) by Kahng and Attala [6] sub-sequentially started the way among other things to the construction of computers, which in the beginning were controlled by punch card and later by keyboard and mouse.
It took another 30 years until E. Neher and B. Sakmann developed Noble Prize wining Patch Clamp Technology [7], which allows recording and stimulating of Ion channels in cells. A major disadvantage of this superb tool is that in the course of the measurement the cells have to be penetrated with a pipette which will lead to the death of the cell.
In January of the year 1985 P. Fromherz, at that time at the University of Ulm, presented the idea of “Brain Online – the feasibility of a neuron silicon junction” at a Winter Seminar in Kloster. [8]

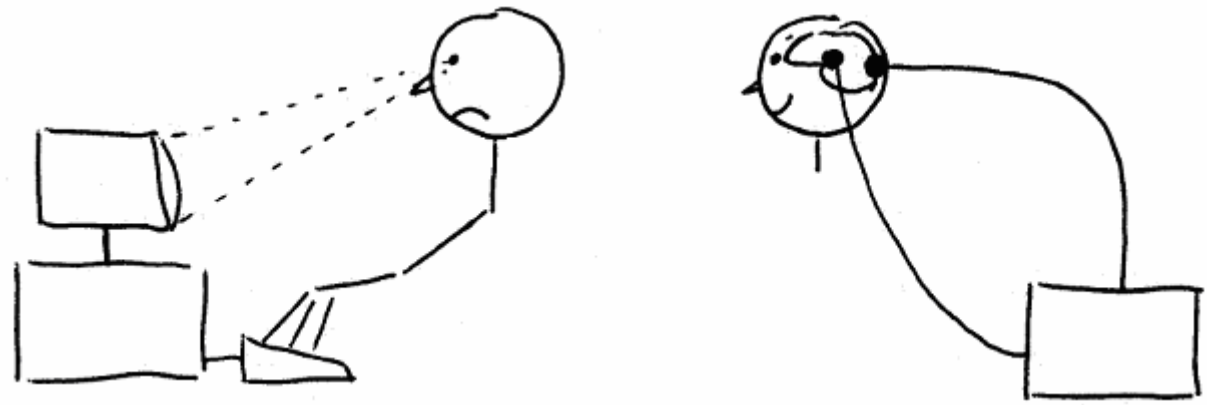

Figure 1: Interaction with the computer – now and in future? [8]

Fromherz stated the possibility of exchanging the macroscopically hand keyboard and eye screen coupling between computer and brain (Figure 1, left) with a direct microscopically coupling (Figure 1, right).
To realize such a hypothesis, Max Plank Institute for Biophysics with Prof. Peter Fromherz as the leading scientist, in their pioneering work, used the conventional Silicon and thermally grown high quality SiO_2 based transistors and electronic circuits to grow living cells on. [9]

Since 1977 on the other hand, a class of materials – *organic polymers* – have been found to be electrically conducting and they are versatile with respect to their processing and device fabrication leading a breakthrough in the field of organic electronics. [10, 11, 12, 13]
Since organic polymers are solution processable and have tunable electrical and optical properties, they are versatile for adaptation to the bio-systems. It is the aim of this thesis to study the feasibility of Cell growth and Culture, investigate the bio-compatibility using various types of organic insulators and conducting polymers. This thesis composes of first hand studies of various organic dielectrics and semiconductors interacting with cells and their electrical and optical properties.

2. Introduction

2.1. Cell-Chip Junction

In principle the Cell Chip junction can be seen as an interface between mostly ion driven signaling and electronically driven signaling/signal processing. A direct coupling of ionic signals in a cell and electronic signals in a microelectronic device can be achieved by electrical polarization.

When the insulating plasma membrane of the cell is in direct contact with the insulating dielectric of the device a compact dielectric should be formed. The electrical field of the polarized cell membrane leads to a polarization of the dielectric which furthermore leads to the formation of a channel between Source and Drain contact embedded in the Semiconductor (Figure 2, top). This would be the reading of a signal from the cell or the controlling of the transistor by the cell.

The other way an electrical field applied to the dielectric of the device (not necessarily a transistor) leads to a polarization of the plasma membrane which furthermore leads to the opening of voltage gated ion channels (Figure 2, bottom). This refers to gating of ion channels by the electronic device.

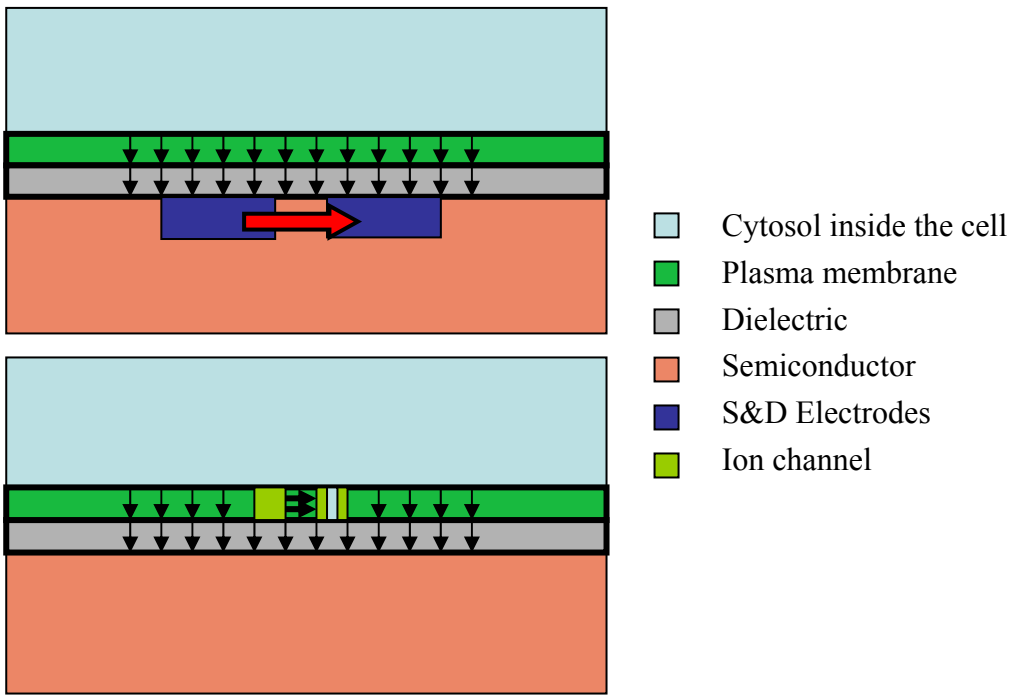

Figure 2: Iono-electronic interfacing by direct polarization (as in [14])

Unfortunately when a cell grows on a dielectric one cannot expect that the two insulating materials form a compact dielectric. As we have heard earlier the cell membrane is not a smooth surface because of proteins and glucose molecules which form the glycocalix (cell coat). This cell coat disallows a tight adherence of lipid membrane and dielectric material, by forming a electrolyte filled cleft between them which shields the electric fields and suppresses a direct polarization of the membrane and dielectric. In this case we can talk about a planar core-coat conductor where the membrane and the dielectric form the coat and insulate the electrolyte from the conducting cytosol and the semiconductor.

Including this to the model the polarization of the membrane leads to ionic and displacement currents inside the electrolyte that gives rise to a so-called Transductive Extracellular Potential (TEP) which can be detected by the transistor under the cell (Figure 3, top).

Again the opposite way also works for stimulating the cell by a polarized dielectric (Figure 3, bottom) which induces a TEP into the electrolyte which then stimulates the voltage activated ion channels, leading to a polarization of the cell membrane. [14]

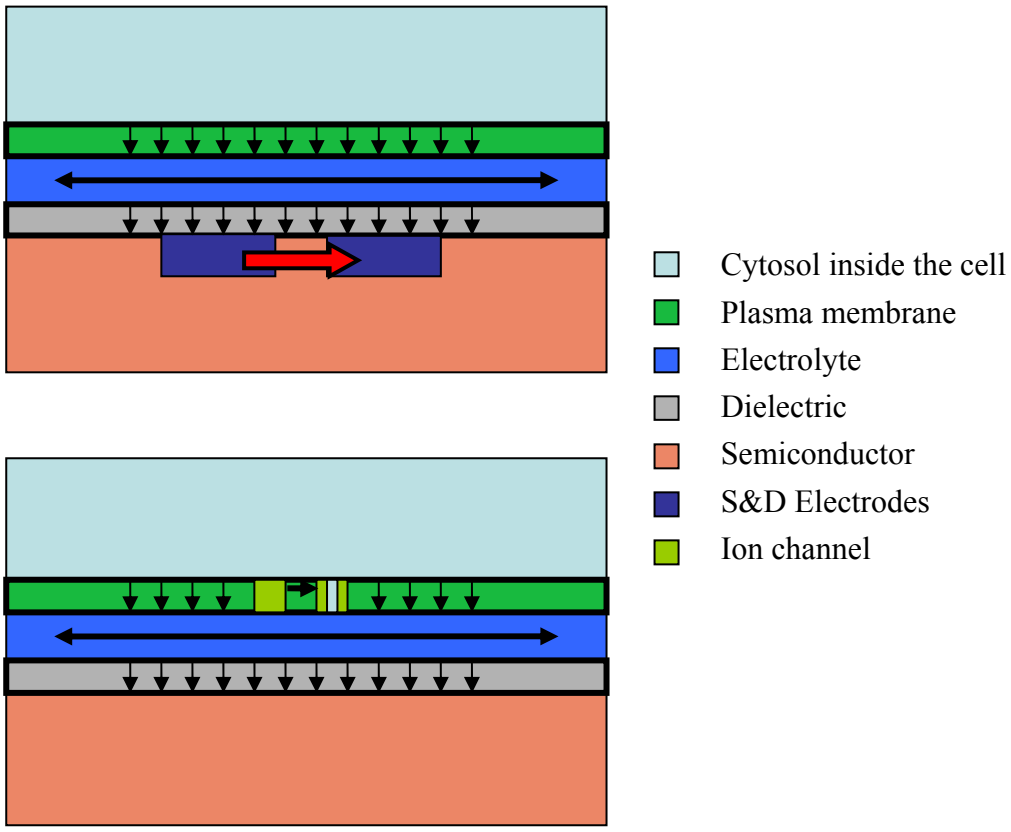

Figure 3: Iono-electronic interfacing by indirect polarization via TEP (as in [14])

The transductive extracellular potential is determined by the current balance in the core-coat conductor of the junction. For the current and the voltage two models have been developed by

the Fromherz group: the spatial resolved area contact model and the more simplified point contact model.

2.1.1. Point contact model

In the simpler point contact model the core-coat conductor can be described by the following equivalent circuit:

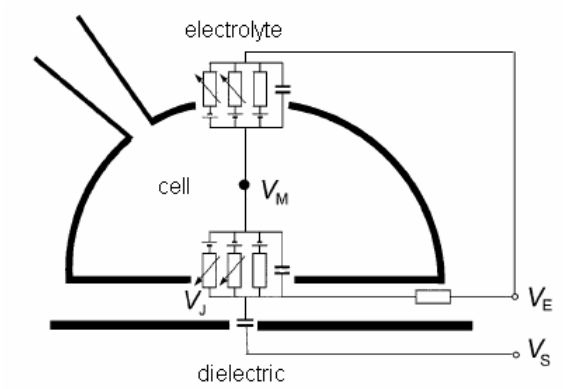

Figure 4: Equivalent circuit for Point Contact Model (taken from [14])

The conductive cleft is represented by a global resistance and the attached membranes are described by their capacitances.

2.1.2. Area contact model

In this model the contact between cell and the dielectric of the chip is represented by a flat, two-dimensional cable: the resistance of the cleft is isolated by the dielectric on the one side and on the other side by the junction cell membrane which is regarded as a second capacity.
The model can be described by the following equivalent circuit:

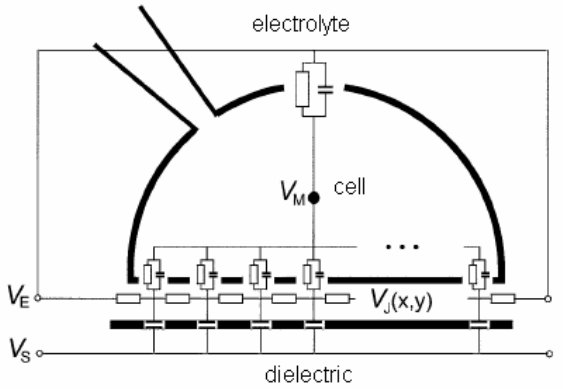

Figure 5: Equivalent circuit for Area Contact Model (taken from [14])

As can be seen in Figure 5 the current is described in each area element by infinitesimal elements of oxide, membrane and electrolyte which are represented as capacitors and Ohmic resistances.

In both models it is essential that the dielectric capacitance and the cell membrane capacitance are very similar because due to Equation 1 the voltage drop over two in series connected capacitances is determined by the smaller capacitance.

$$\frac{1}{C_{eff}} = \frac{1}{C_S} + \frac{1}{C_M}$$

Equation 1: Capacitance in series

The capacitance of a cell membrane is estimated to be in the order of 1μF/cm^2, derived from a dielectric constant ε = 5 and a thickness of the membrane of about 4 nm using the geometrical capacitance Equation 2.

$$C = \frac{\varepsilon\varepsilon_0 A}{d}$$

Equation 2: Geometrical capacitance

The Fromherz group usually designs their chips with a 10 nm thick SiO_2 layer so that they obtain a SiO_2 dielectric capacitance of 0.34μF/cm^2 ($\varepsilon_{0,SiO_2} = 3.9$). For organic dielectric layers such high numbers are hard to reach because it is hard to achieve such thin films as can be seen in the experimental section (3.4).

2.2. Signaling in Biology

The communication between cells is mainly done by the exchange of molecules. This can happen by messaging molecules like cAMP. cGMP, IP3 (2^{nd} messenger) or by ion flux, which activate all kinds of processes inside a cell and are also responsible for nerve impulse transport.

As this thesis is aiming for a possible interface between organic materials based information technology and biology, messaging will be done by ion flux, not with 2^{nd} messengers. To explain how signalling works in cells we start from the beginning.

2.2.1. The Cell

The cell is the structural and functional unit of all living organisms [15], and is sometimes called the "building block of life." Small organisms like bacteria, consist just of a single cell whereas other organisms, such as humans have an estimated 100 trillion or 10^{14} cells. The size of cells varies from a 2µm up to 200µm.

In large organisms the cells have specified to certain responsibilities, like neurons, skin cells or sperm cells. Despite this high specialisation there are some features common to all cells: [16]

- Cell organelles are contained within a cell surface membrane.
- Reproduction by cell division.
- Cells can take up raw material, build cell components, convert energy and molecules and release the by-products. The functioning of a cell depends upon its ability to extract and use chemical energy stored in organic molecules.
- Respond to external and internal stimulus, like pH or temperature change.
- Decoding of DNA genes and production of proteins and enzymes.

Derived from the Latin word *cellula*, a small room, the cell contains all necessary organelles inside a hull, the plasma membrane (Figure 6).

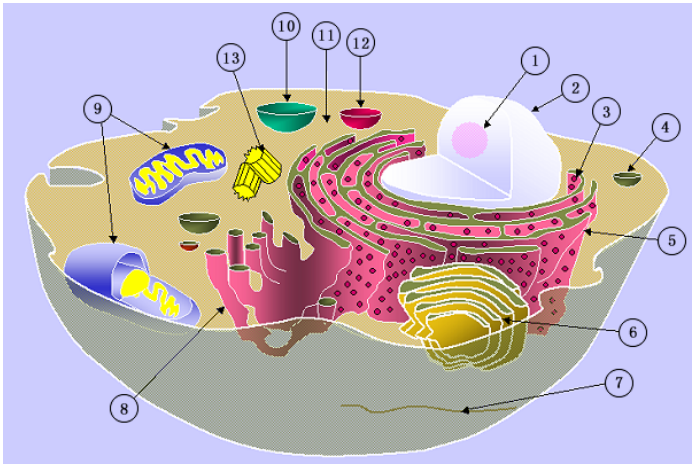

Figure 6: The Cell (taken from [17])

(1) Nucleolus, (2) Nucleus, (3) Ribosome, (4) Vesicle, (5) rough Endoplasmic Reticulum (ER), (6) Golgi apparatus, (7) Cytoskeleton, (8) smooth ER, (9) Mitochondrion, (10) Vacuole, (11) Cytoplasm, (12) Lysosome, (13) Centriole

2.2.2. The plasma membrane

As seen above, a living cell is a collection of organelles which are enclosed in a hull, the so-called plasma membrane. The Plasma membrane has a barrier function, that means it has to keep all the organelles inside the cell and it has to prevent other molecules from entering the inside of the cell. Beside this barrier function the membrane must also be permeable for nutrients and waste for which the membrane is interspersed with channels and pumps.

The basic structure of the Plasma membrane consists of a bilayer of phospholipids (Figure 7) which have a hydrophilic head group and a hydrophobic tail. In aqueous media they form a bilayer where the hydrophobic tails face themselves and the hydrophilic head groups face the media.

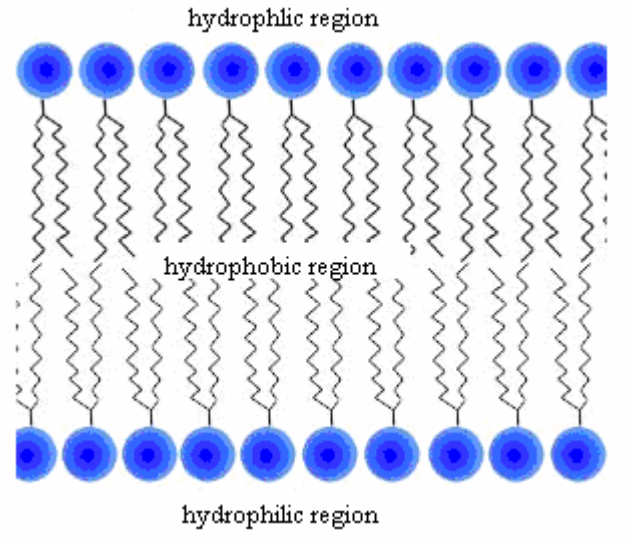

Figure 7: Lipid bilayer membrane (taken from [18])

The four major classes of phospholipids for structural use are phosphatidylcholine (PC), phosphatidylethanolamine (PE), phosphatidylserine (PS) and sphingomyelin (SPHM) (Figure 8).

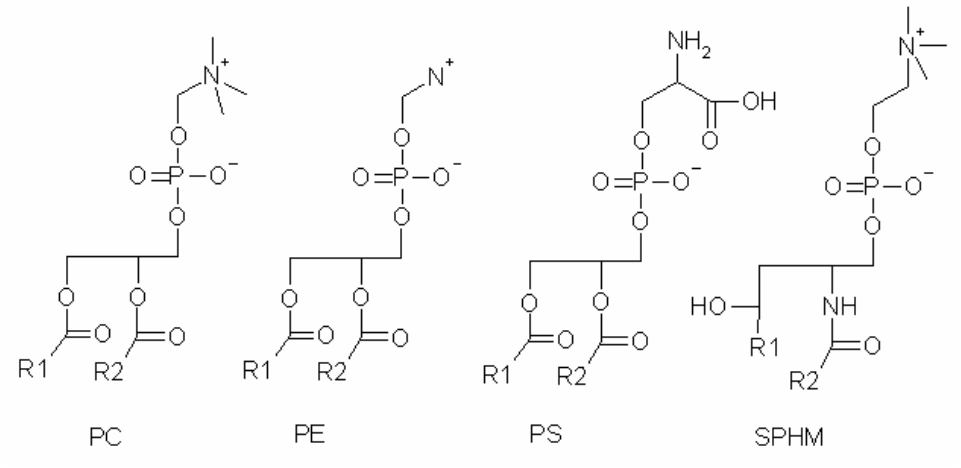

Figure 8: Phospholipids PC, PE, PS, SPHM

The extra cellular side of the membrane has additionally glycolipids (glucose or oligosaccharides are covalently bound to lipids) which then form an asymmetrical bilayer and a protective cover the so-called glycocalix (cell coat). This coat protects the cell and also mediates the adherence of cells to various surfaces.

One of the essential parts of the cell membrane is the barrier function where the hydrophobic middle part of the bilayer plays an important role. Small and hydrophobic molecules like O_2 or CO_2 are just diffusion limited, whereas big molecules are space limited and charged molecules and ions (K^+, Ca^{2+}, Na^+, Cl^-) are not allowed to pass because of their charge. Being impermeable for a lot of important messaging molecules and nutrition the cells have developed specialized proteins which help to transport these molecules and ions.

Beside Transport functions membrane proteins have also other functions (Figure 9):

- connection proteins
- receptor
- enzymatic catalysis of reactions

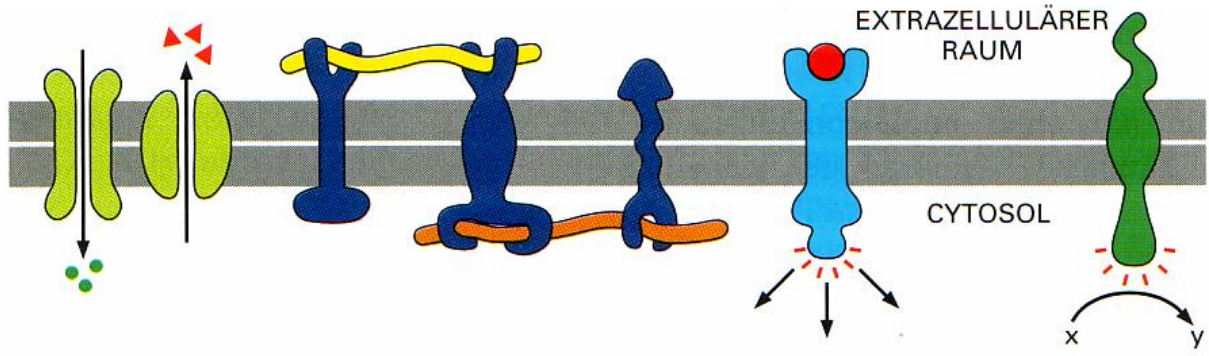

Figure 9: Use of transmembrane Proteins: transport, connections, receptor and enzymatic catalysis (taken from [16])

2.2.3. Membrane transport:

To transport nutrition like sugars and amino acids inside the cell and waste out of the cell, as well as to regulate the intracellular concentration of ions, the membrane is blotched with transmembrane transport molecules. Bigger molecules are usually transported with vesicles (Figure 10).

Vesicles are formed when lipids gather around the big molecule and form a ball. This ball can fuse with the membrane and release the molecule to the outside of the cell.

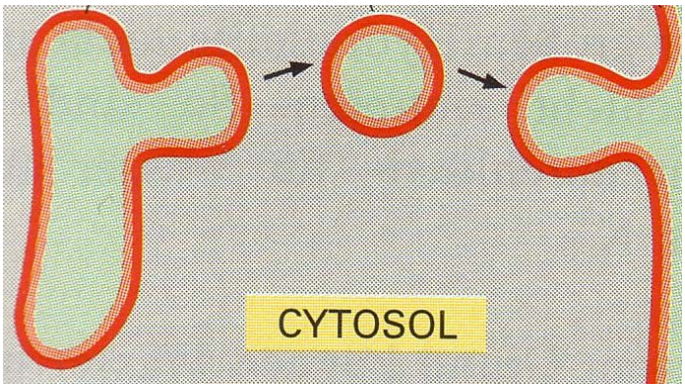

Figure 10: Transport with the help of vesicles (taken from [16])

Transport with transmembrane transport proteins:

Transmembrane transport proteins usually consist of a long polypeptide chain that crosses the membrane more than once (multipass – transmembrane protein). The protein is folded to α-helices and forms a pore through the membrane, whose structure can be clarified fully by x-ray crystallography structure analysis [19], e.g.: Bacteriorhodopsin (Figure 11)

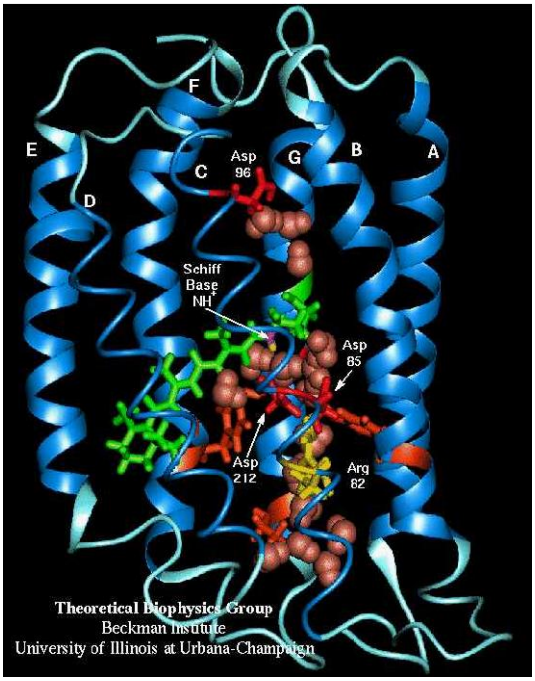

Figure 11: X-Ray crystallographic structure analysis of transmembrane protein Bacteriorhodopsin (taken from [20])

Transmembrane transport proteins can be sorted in two classes: Carrier proteins and channel proteins:

2.2.3.1. Carrierproteins:

Carrierproteins bind the dissolved molecule on one side of the membrane and transport it to the other side by changing their conformation. This can be compared with a turnstile: one molecule after the other binds to binding site, the conformation changes and the molecule unbinds on the opposite side of the membrane. The transport is highly selective due to direct binding of protein and transported molecule.

Transport is passive, when the transport occurs along the concentration gradient or active when it is against the gradient. Active transport requires input of energy in form of light, ATP reduction or the energy comes from a passive transport of another molecule in the same carrier protein (coupled transport, ion pumps, Figure 12)

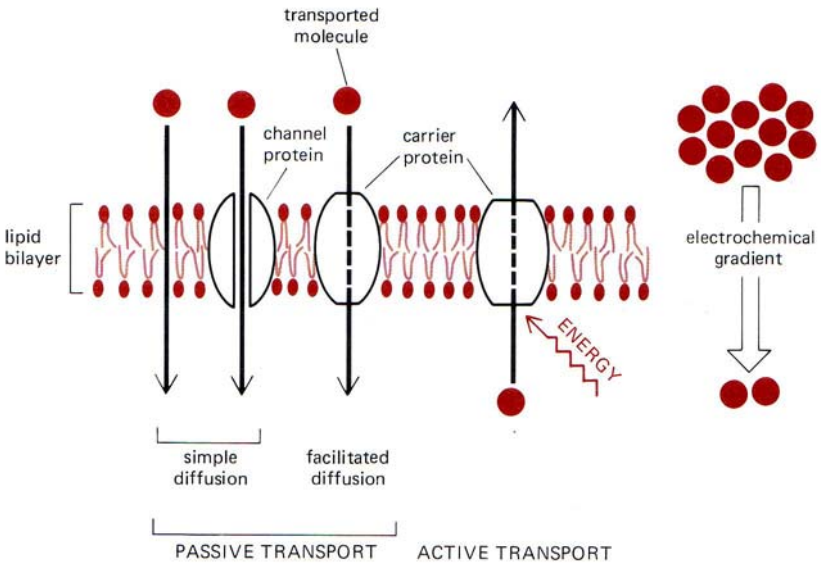

Figure 12: Possibilities for transmembrane transport (taken from [21])

2.2.3.2. Ion Channels

Ion channels are water filled pores build by one or more membrane proteins (so-called sub units α, β, γ and so on) through the membrane, which are ion selective (Cl^-, Na^+, Ca^{2+} and K^+ channels are known) and most important not open all the time, but regulated by different mechanism [22,23].

Usually the α subunit has most of the functional properties whereas the other subunits control the structure and activity of the α subunit. Within the α subunit a unit of 300 - 400 amino acids is repeated 4 times, each repeated unit contains 6 transmembrane domains and each of the 4 repeated units has a gating mechanism (not necessarily a voltage gated as seen in Figure 13, the yellow transmembrane tube). The four repeat units are arranged circular to form the water filled pore (Figure 15).

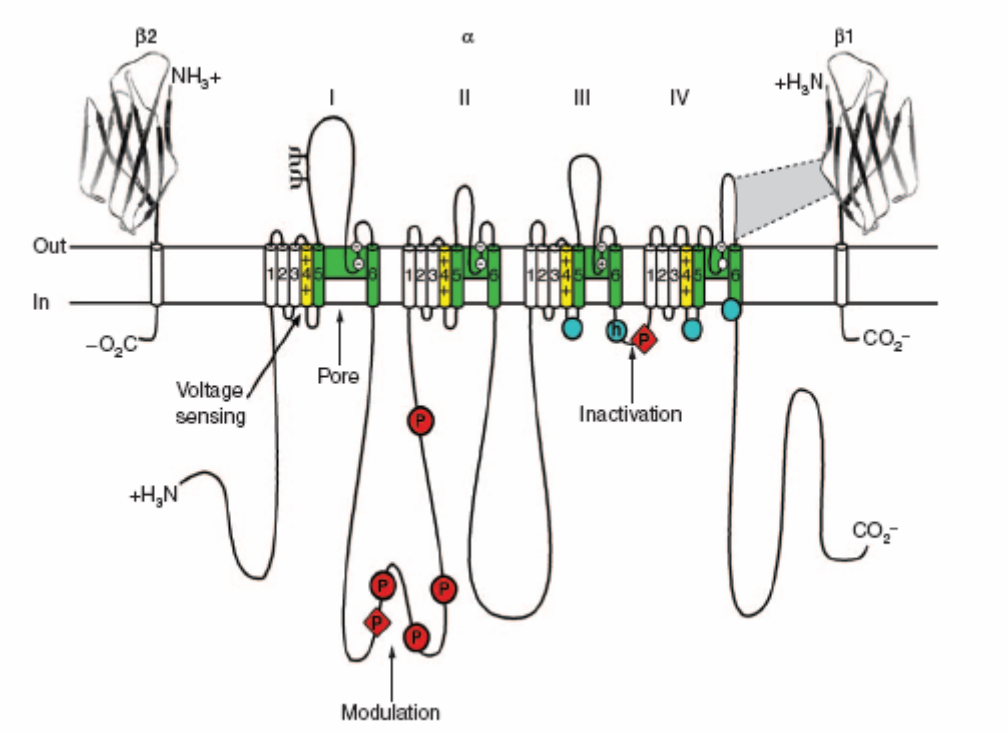

Figure 13: Voltage gated sodium channel (taken from [24])

Important is here to say that the transport can only happen along the concentration gradient. Ion selectivity is achieved by size exclusion and matching of the charges. Ion transport through ion channels is approximately 1000 times faster than with carrier proteins and leads to a fast change of the membrane potential.

Opening of an ion channel can be achieved by three different gating mechanisms:

- Ligand gated ion channels (LGIC)
- Stretch and heat activated ion channels
- Voltage gated ion channels (VGIC)

Ligand gated ion channels (LGIC):

These types of ion channels are regulated by a neurotransmitter such as nicotin, acetylcholine (well known nicotine – acetylcholine receptor channel, nAChR) or even single ions. The neurotransmitter receptor, which is a part of one of the transmembrane proteins, can be localized on the outside of the membrane or on the inside. When the neurotransmitter binds to the receptor, the transmembrane proteins change their conformation which allows ions of one kind to pass the channel.

Stretch and heat activated ion channel

Stretch and heat activated ion channels respond either to a mechanical deformation of the plasma membrane or to a conformation change due to heat. An example is the pressure sensitive ion channel inside our ear, which react to the movement of the fine hair attached to them. (Figure 14) [25]

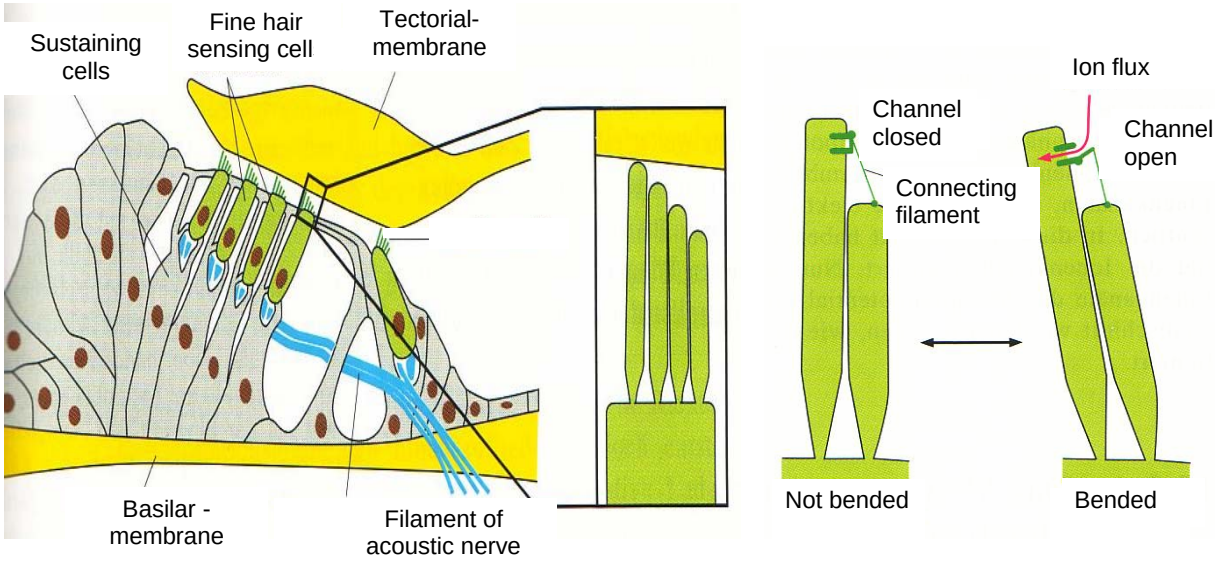

Figure 14: Pressure sensitive ion channels enable to hear (taken from [16])

Voltage gated ion channel (VGIC)

Voltage gated ion channels are regulated by an electrical potential difference around the channel. Voltage gated ion channels have a crucial role in signal propagation in neurons, but they are also very common in other cell types.

As other channels, the voltage gated sodium and calcium channels consist of one long polypeptide chain which surpasses the membrane up to six times (α helices S1-S6) and has the voltage sensor located usually at the S4 domain which has positively charged amino acids residues at certain positions which allow only one kind of ions to pass the channel.

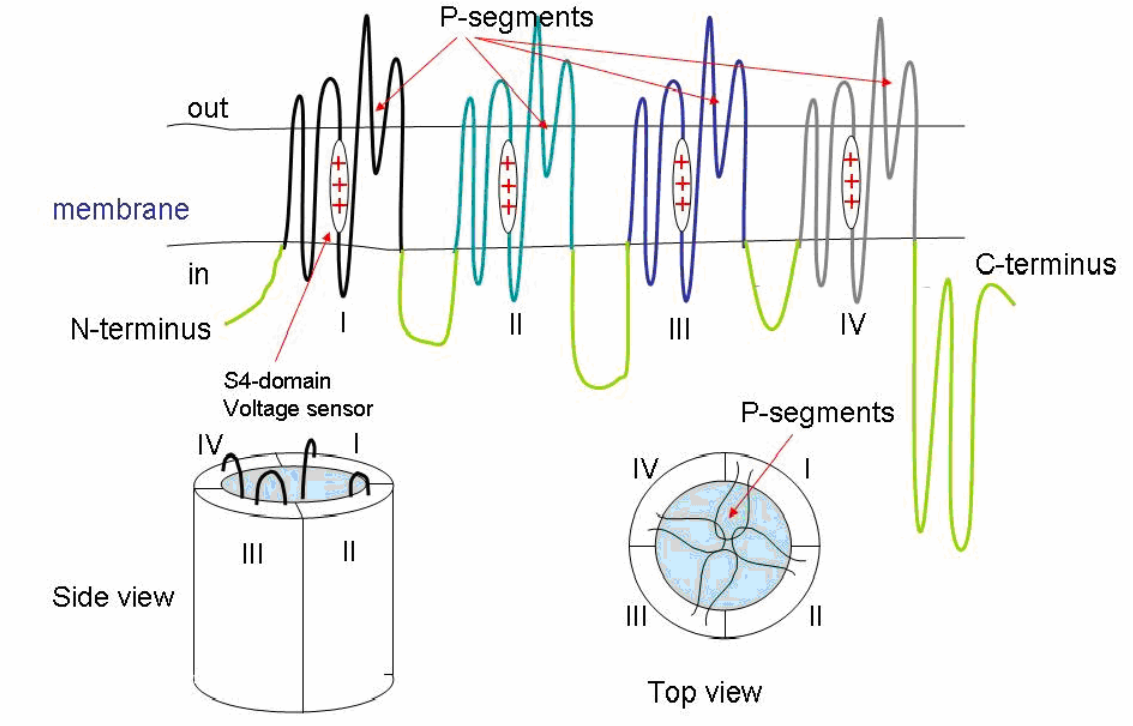

Figure 15: Voltage gated calcium channel (taken from [26])

In this thesis a L-type Ca^{2+} channel has been used, because calcium ions are particularly important in eukaryotic cells, controlling and regulating a number of processes, like activation of gene expression or muscle contraction.

2.3. Signaling in Information Technology

As mentioned before, this thesis wants to show the possibility of an interface between organic materials based information technology devices and cells. Therefore the basic electrical/electronical devices which maybe used for this kind of interfaces are: a capacitor and a transistor

2.3.1. The (organic) capacitor

In general the capacitor is an electrical device that can store energy in the electric field *E* between two conductors (plates, area *A*) at a distance *d*. The room between the plates is filled with an insulator. When voltage is applied to the device, electric charges of equal magnitude, but opposite polarity, build up on each plate $+Q$, $-Q$ [27]

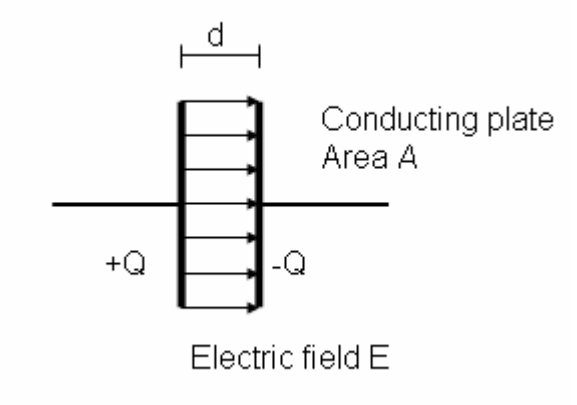

Figure 16: The capacitor

The capacitance *C* is a value for the amount of charges stored in the capacitor for a given voltage.

$$C = \frac{Q}{V}$$

Equation 3: Capacitance

The capacitance of a two plate capacitor can also be derived from its size and kind of dielectric (geometric capacitance):

$$C = \frac{\varepsilon \varepsilon_0 A}{d}$$

Equation 4: Geometrical Capacitance

Where ε is the permittivity of the dielectric between the two metal plates and ε_0 is the vacuum permittivity (ε_0 = 8.8541878176 × 10^{-12} F/m), d is the thickness and A the area of the capacitor. Values for ε in organic materials are typical in the order of 1to 10 (e.g. PVA ~ 8).
To achieve high capacitance per unit area one can either vary the material itself and therefore have different permittivity constants or change the thickness of the materials. As the permittivity constants of organic dielectrics are in the same range and even higher than that of SiO_2 the thickness of the organic dielectric will be a crucial part to obtain high capacitance per unit area values which can be used in a cell – chip junction.
Typical organic dielectric can be seen in figure 16:

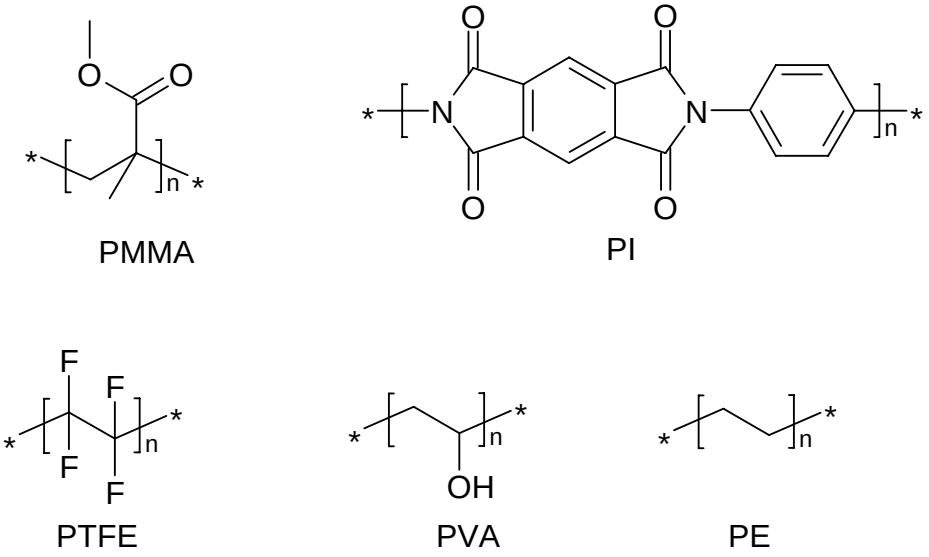

Figure 17: Common organic dielectrics: Polymethamethacrylat (PMMA), Polyimide (PI), Polytetraflourethylene (PTFE), Polyvinylalcohol (PVA), Polyethylene (PE)

To measure Capacitance usually a LCR meter is used.

2.3.2. Working principle of LCR meter

When measuring impedance or derived values like capacitance and resistance with a LCR meter, the measurement can be described by an equivalent circuit as seen in Figure 18. The current flowing through the device under test (DUT) also flows through a resistor R. At the point L the potential is kept at zero volts (virtual ground), because the current through R balances with the DUT current by operation of the I-V- converter amplifier. The DUT impedance is calculated by the voltage at point H (U_{out}) and the voltage drop over R (U_R). [49]

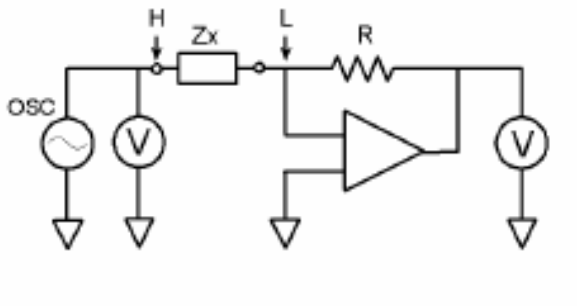

Figure 18: Equivalent curcuit for LCR measurement (taken from [49])

Measurement values are only the real parts of U'_{out} and U'_R and the imaginary parts of U''_{out} and U''_R. From these values the Impedance (Equation 5) and the angle θ (Equation 6, Figure 19) are calculated:

$$Z_{out} = R\frac{U'_{out} + iU''_{out}}{U'_R + iU''_R}$$

Equation 5: Impedance calculation

$$\theta = \tan\frac{U''_{out}}{U'_{out}}$$

Equation 6: Phase Angle θ

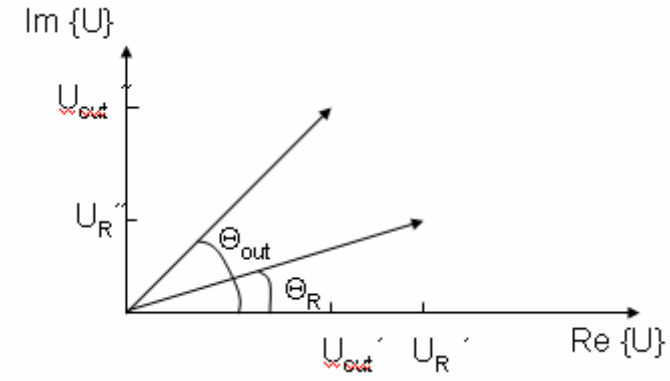

Figure 19: Angle *θ* in Impedance measurement

From the Impedance the Capacitance is derived using the following Equation 7:

$$Z = \frac{1}{i\omega C}$$

Equation 7: Capacitance – Impedance correlation

For further experiments one electrode of the capacitor will be the cell, which should enable us to stimulate [28], [29] or read a signal from the cell. As the amplitude of the signals from the cells is considered to be very small, amplification will be necessary, which can be easily obtained by a transistor.

Before explaining the organic field-effect transistor one should explain how organic polymers can be semi-conducting.

2.3.3. Organic Semiconductors

Semiconductors in general are compounds whose conducting properties are somewhere between those of a metal and an insulator. The conductivity and other electrical properties of semiconductors are determined by the material's electronic band structure. These electrical properties may be modified by introducing impurities in a process known as doping. Till the already mentioned discovery of organic semi conducting polymers by H. Shirakawa, A.G. MacDiarmid and A.J. Heeger in 1977, this property was attributed to inorganic materials like Germanium and Silicon.

The materials can be doped in various ways (Figure 20):

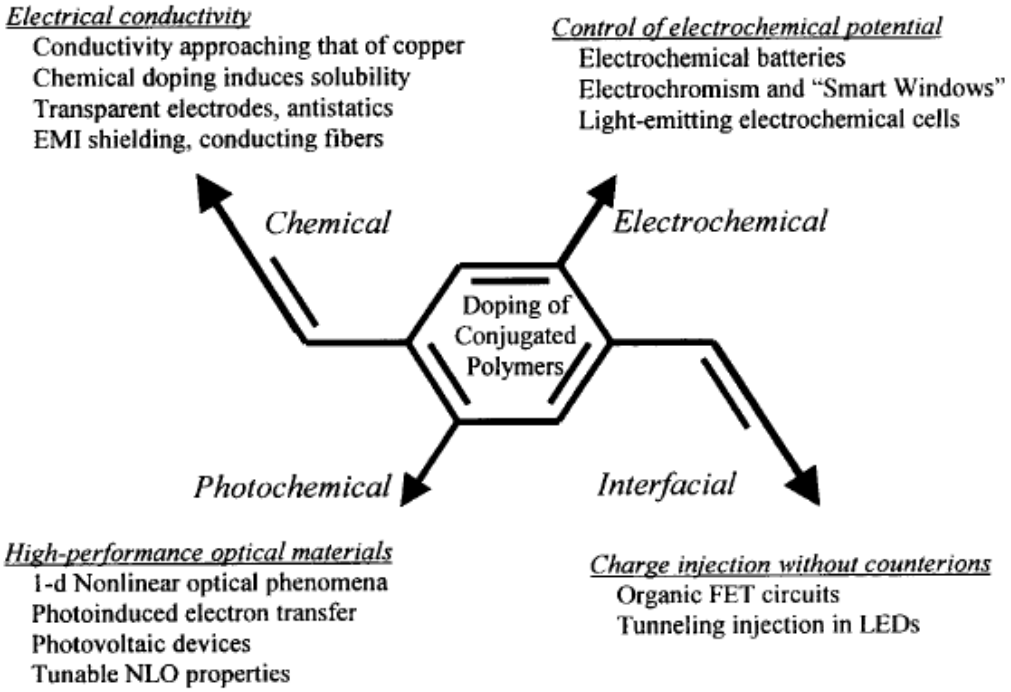

Figure 20: Doping mechanism and related applications (taken from [13])

As can be seen in Figure 20 *interfacial doping* of conjugated polymers is a way to obtain organic field-effect transistors, which means that electrons and holes are injected from metallic contacts into the π* – and π – bands (LUMO & HOMO), respectively:

- Hole injection into a already filled π – band:

  $(\pi - \text{polymer})_n - y(e^-) \Rightarrow (\pi - \text{polymer})_n^{+y}$

- Electron injection into an empty π* – band:

  $(\pi - \text{polymer})_n + y(e^-) \Rightarrow (\pi - \text{polymer})_n^{-y}$

Hole and electron injection at the metal semiconductor interface leads to oxidation or reduction of the polymer but the polymer is not doped in the sense of chemical or electrochemical doping because there are no counter ions present. [13]

Today a bright variety of semiconductor materials is known like those in 21 which have been used in this thesis.

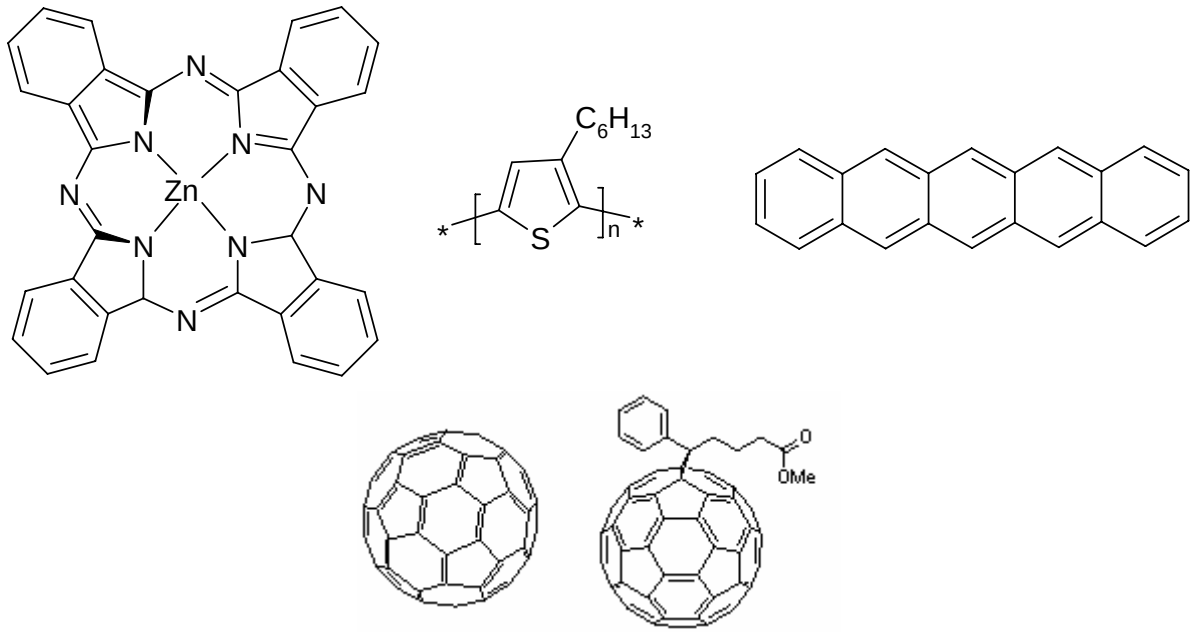

Figure 21: Used semiconductor materials: ZnPc, P3HT, Pentacene, C_{60} and PCBM

2.3.4. The (organic) field-effect transistor

The basic element of a metal oxide semiconductor field-effect transistor (MOSFET, Figure 22) is a capacitor. One plate is formed by a conducting channel between two ohmic contacts – source and drain electrode. The second plate is the gate electrode that modulates the conducting channel when a gate voltage is applied, which creates an electrical field perpendicular to the substrate plane.

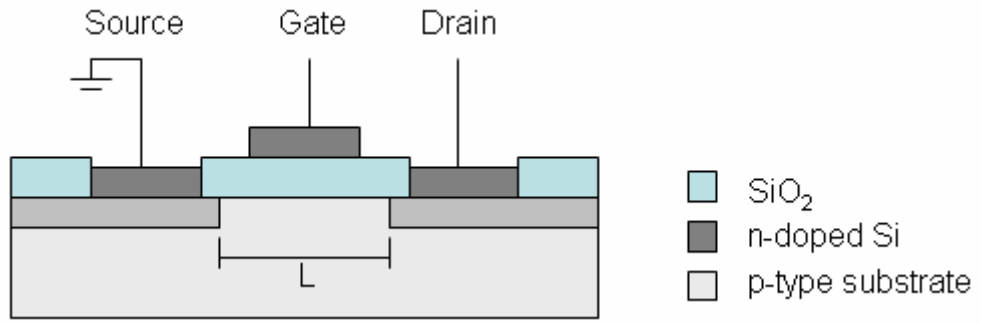

Figure 22: MOSFET structure with p type semiconductor substrate (as in [33])

Based on the concept of the MOSFET, the first organic field-effect transistor (OFET) was reported by Koezuka [30] and co-workers in 1986 using polythiophene as semiconductor and a thin film transistor (TFT) structure (Figure 23).

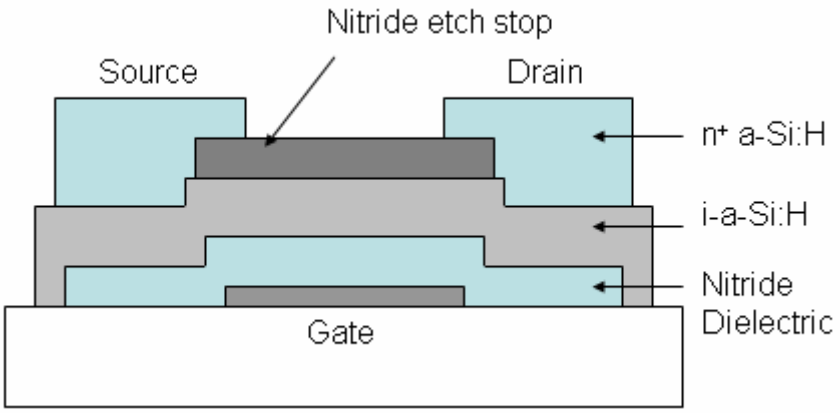

Figure 23: a-Si:H thin film transistor (as in [33])

Apart from the above shown MOSFET and TFT structures a few other structures are known for organic field-effect transistors [31]:

- Bottom gate, top contact structure (BG/TC, Figure 24a)
- Bottom gate, bottom contact structure (BG/BC, Figure 24b)
- Top gate, bottom contact structure (TG/BG, Figure 24c)
- Top gate, top contact structure (TG/TC, Figure 24d)

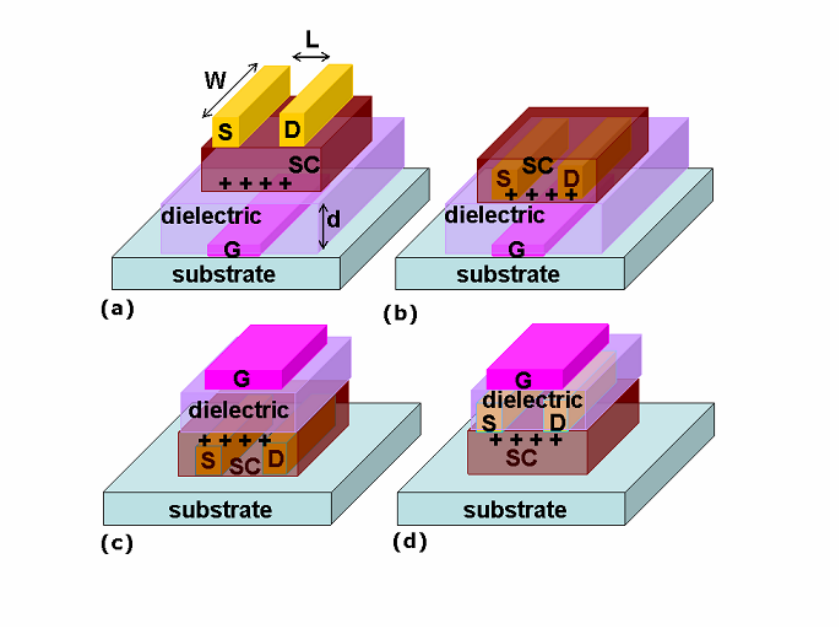

Figure 24: Schematic Device structures (taken from [31])

For applications with cells, the metal gate of the top gate transistor will be replaced by the cell culture as it has been shown already by the Fromherz group on Si-based field-effect transistors [32].

2.3.5. Operating principle of OFETs

The simplest way to describe the OFET operating principle is to use energy level diagrams including the Fermi level of the source/drain metal electrode and the HOMO/LUMO level of the semiconductor. When the applied gate voltage is equal to zero (Figure 25, left) the intrinsically undoped organic semiconductor will not show any charge carriers. Small currents (due to large distance between the electrodes and a high resistance of the organic semiconductor) can be obtained by applying a voltage to the drain electrode (direct injection of carriers to the semiconductor).

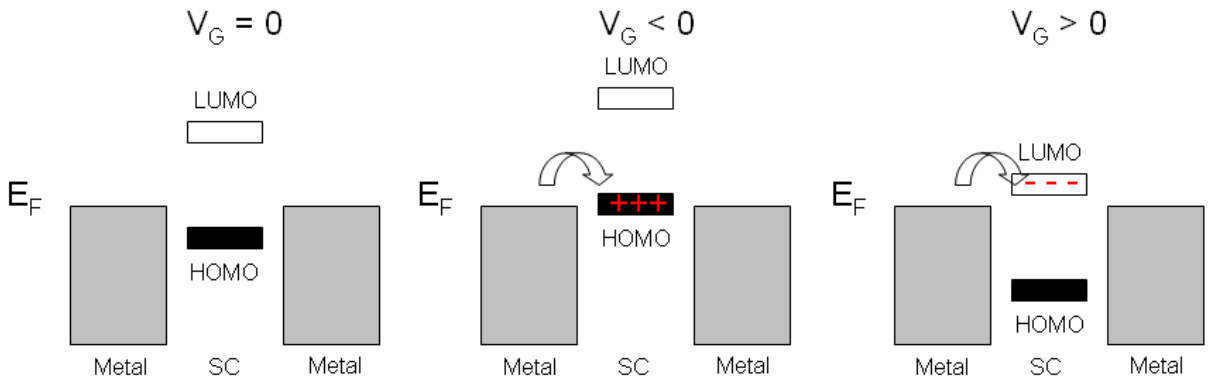

Figure 25: Working principle of OFET with respect to applied gate voltage V_G (taken from [31])

When applying a negative voltage to the gate electrode (Figure 25, middle), positive charges (holes) are induced at the interface between organic semiconductor and dielectric. If the Fermi level of the metal source/drain electrodes is also close to the HOMO level of the organic semiconductor holes can be injected from/to the metal to/from the HOMO of the organic semiconductor by applying a voltage V_{ds}. In this combination of metal and organic semiconductor only positive charges can be transported and it is termed p-type semiconductor.

To get a n-type semiconductor, a positive voltage applied at the gate electrode induces negative charges into the interface (Figure 25, right), which then can be extracted if the Fermi level of the metal source/drain electrodes is close to the LUMO of the organic semiconductor.

The accumulated charge carrier density in the channel region is a decisive parameter for organic field-effect transistors because the transport through the channel is heavily influenced

by the interface of the organic dielectric and the semiconductor. The basic device parameters for modelling of organic field-effect transistors are the properties of the insulating layer, the channel length L, which is the distance between the two metal electrodes and the thickness of the semi conducting layer W (Figure 24).

3. Experimental

3.1. Compatibility test

Before any cell-chip devices can be build one has to ensure that the cell actually likes to adhere on the surface. To test the cell compatibility all materials were spin coated or vacuum deposited on 30 mm diameter untreated, cleaned glass cover slides.

3.1.1. Sample Preparation

To ensure best adherence of dielectric or semiconductor materials the 30 mm glass cover slides were in a first step cleaned in a 2 % solution of *"Hellmanex"* (purchased from Hellma GmbH) in water in the ultrasonic bath. After 15 minutes or longer the cover slides were washed with de-ionized water, ethanol and again with water. The ethanol washing step was inserted to ensure that the cover slide is free of any living materials like bacteria and fungi, to make sure the applied cell culture is not contaminated.

Spin coating was done with the standard spin coating program used in our laboratory: the sample holder was accelerated within 4 seconds to 1500 rounds per minute kept at this speed for 40 seconds and further accelerated to 2000 rpm and held there for 20 seconds before slowing down. Spin Coating was either done inside the argon glove box (MBraun) for air sensitive materials or outside the glove box for all other materials.

Evaporation of small molecule semiconductor was done in our laboratory's Leybold UNIVEX multi source evaporation machine.

3.1.2. Sterilization

All samples were kept inside in a sterile laminar flow-box under UV irradiation over night to ensure a sterile surface before the cells were seeded.

3.1.3. HEK293 cell line

Human Embryonic Kidney Cells are adhering fibroblast-like cells, growing mostly in monolayer, which have their origin in primary kidney tissue that was transformed with Adenovirus AD5 by F. Graham and co-workers at McMaster University in 1977. [34] HEK293 cells have a doubling time of 20 to 24 hours and are kept in a medium containing 90 % Dulbecco's Modified Eagle Medium (DMEM), 10 % Fetal calf serum (FCS) and some

antibiotics (for Ingredients of DMEM see 8.1Appendix A). The HEK293 cell line is well established and well characterized throughout the scientific community.
Usually this type of cells adheres within the first five hours to the surface. After this they continue to reproduce themselves. In case of not adhering to the surface the cells cluster to big clouds of cells, so that they feel like adhering and start reproducing.

3.1.4. Cell culturing

Cells were cultured in DMEM in an incubator at 37 °C and 98 % humidity in air, containing 5 % CO_2 over night before the result of the cell culturing was checked by light microscopy on the next day.

3.1.5. Tested materials

The following dielectric and semiconductor materials have been investigated if they are compatible with the HEK293 cell line.

3.1.5.1. Dielectrics

Divinylsiloxanebis-b*enzocyclobutene* (BCB, Cyclotene™) [35] obtained from Dow Chemicals was spin coated as received. During the thermal cure at 250 °C for 30 minutes under a 20 mbar Ar atmosphere the following reactions happen to the monomer:

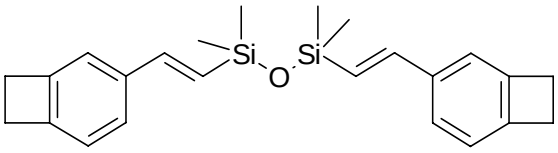

Figure 26: BCB monomer

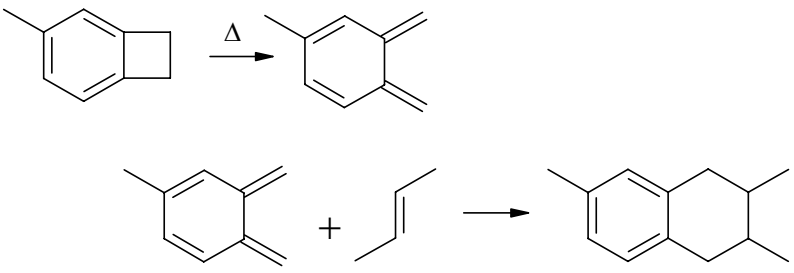

Figure 27: BCB crosslinking reaction

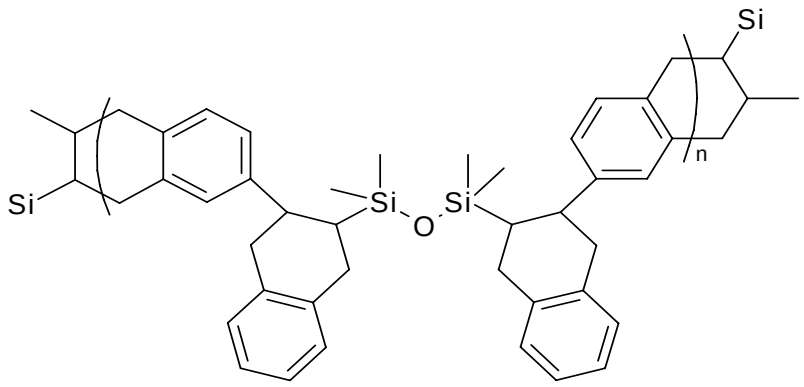

Figure 28: Thermally cross linked BCB

Polyimide (Kemitite^{TM} CT4112, PI) was obtained from Kyocera Chemicals Corp. and used as received (Polyimide precursor polyamic acid in N-methylpyrolidon) [36]. The spin coated films were first heated to 75 °C for 30 minutes to avoid strong shrinking of the film, before heating to 180 °C for one hour.

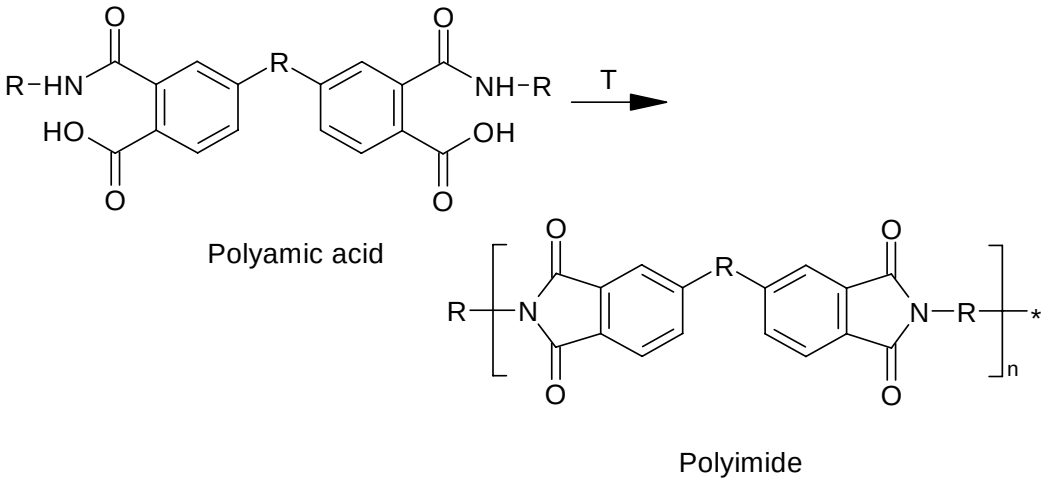

Figure 29: Thermally cured polyimide

Since *Polyvinylphenol* (PVP) is water soluble and can therefore not be used as a surface for cells, the PVP was crosslinked with methylated poly (melamine-co-formaldehyde) [37]. As a solvent 1, 2-Propanediol monomethyl ether acetate (PMA) was used. The spin coated film was annealed at 190 °C for 30 minutes.

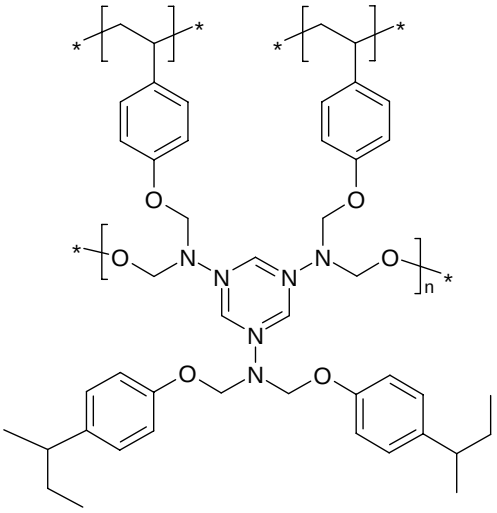

Figure 30: Crosslinked Polyvinylphenol

Polymethylmetacrylat (PMMA) was dissolved in n-butylacetate as received from Aldrich to get an 10 % solution which then was spin coated with the standard spin coating program.

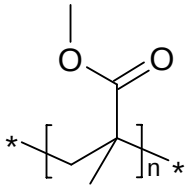

Figure 31: PMMA

DNA-CTMA

The DNA used for this research was purified salmon DNA provided by the Chitose Institute of Science and Technology (CIST). In the production process milt and roe sacs from frozen salmon were homogenized, enzymatically treated, decoloured and filtered and precipitated by adding acetone. The original molecular weight was measured to be 8.000.000 g/mol using gel phase electrophoresis but was reduced to 300.000 g/mol by breaking bonds with ultrasonic. This state DNA was water soluble and therefore not usable for cell growth tests. It was ion exchanged with cetyltrimethylammonium chloride to from a water insoluble material. [38, 39] The DNA-CTMA complex was dissolved in n-butanol and spin coated from a 3 % solution.

Polyethylene (PE) was obtained as ultra high, high and low density polyethylene (UHDPE, HDPE, LDPE) from Borealis and dissolved in 140°C hot decaline. [40] Glass cover slides were preheated to 120 °C prior to spin coating and cooled down after spin coating on the hot plate. Nevertheless film quality was extremely bad, so that not enough samples could be made to test the cell growth.

Cyanoethylpullulan (CyEPl) [41] is the converted product of pullulan, a polysaccaridic polymer which is gained by micro organism. The chemical structure of pullulan depends on the carbon source, the producing organism (different strains of Aureobasidium pullulans) and fermentation conditions. Basic structure consist of 3 α-1,4-glycosidic bond glucose molecules forming the maltotriose unit, which then is α-1,6-glycsidic bond to other units. Up to 10 % Maltotetrose units and a-1,3-glyocosidic bonds are also possible depending on above mentioned conditions. [42]

Pullulan is reacted with acrylonitril to get CyEPl, which was obtained from Shin Etsu Chemical Co. Ltd. The material has a good solubility in various organic solvents, like N-methylpyrolidon (NMP), which was used in this study to spin coat the CyEPl.

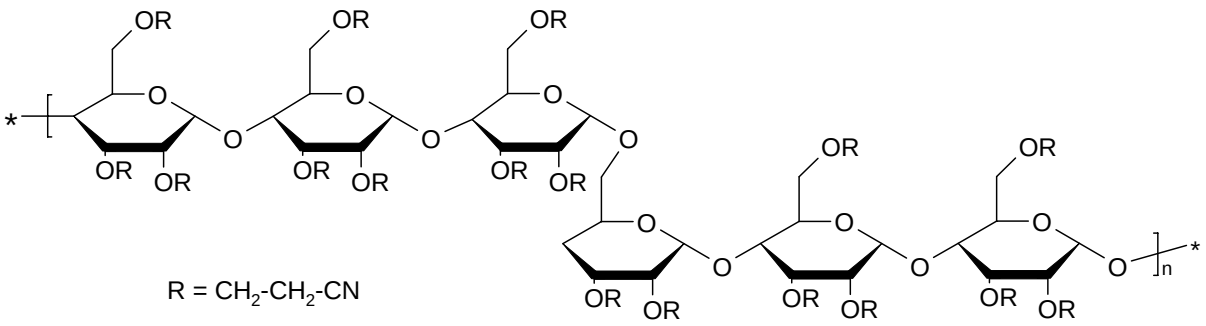

Figure 32: CyEPl

Polystyrene (PS) was obtained from Aldrich and dissolved in chlorobenzene to get a 10 % solution, which was then spin coated onto the cover slides.

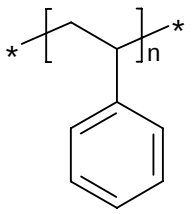

Figure 33: Polystyrene

PDMS: Sylgard® 184 Base (Tetra(trimethylsiloxy)silan) and Sylgard® 184 Curing Agent (Tetramethyltetravinylcyclotetrasiloxane) were obtained from Dow Corning and mixed 1:10 by volume. After spin coating the films were thermally cured at 125 °C for twenty minutes according to the manufacturer instruction [43]

Polyelectrolyte: PEO:$LiClO_4$

Motivated by the extremely large capacitance per unit area (5 μF/cm^2) of this material both Polyethyleneoxide (PEO) and Lithiumperchlorate ($LiClO_4$) were used as obtained from SigmaAldrich and dissolved in acetonitril to achieve a 16:1 ether oxygen-to-lithium ion stoichiometric ratio [51].

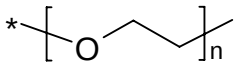

Figure 34: Polyethyleneoxide

During the experiments it was discovered that the PEO:$LiClO_4$ film is highly water-soluble and therefore the cells didn't grow on the film but onto the glass slide after the film had dissolved in the aqueous media of the cell culture. Therefore no pictures will be shown in the results section. (4.1)

3.1.5.2. Semiconductors

Regioregular P3HT (*Poly-(3-hexylthiophene-2, 5-diyl)*) films were prepared by spin coating from a 3 % in Chlorobenzene solution. P3HT was used as obtained from Riecke Metals

ZnPc (*zinc phthalcyanine*) was deposited with Leybold UNIVEX350 vacuum evaporation machine, where the nominal film thickness was set to 100 nm. The material was obtained from Sigma Aldrich and purified by sublimation prior to use.

100 nm *pentacene* were also deposited with UNIVEX350 vacuum deposition machine. The material was used as obtained from Aldrich

C_{60} was used as obtained from MER Corp. and was also deposited with UNIVEX350 vacuum deposition machine.

PCBM (*[6,6]-phenyl C_{61}-butyric acid methyl ester*) is the soluble derivative of C_{60} and was spin coated from 20 – μm filtered 3 % Chlorobenzene solution. Material was used as obtained from Nano-C.

3.1.6. Light microscopy

Light microscopy was carried out on inverted microscope fabricated by Nikon (Eclipse TE200). Digital Imagine was done by a SENSICAM CCD camera.

3.1.7. Pre-treatment of dielectric surfaces

To increase the adhering of cells to the dielectric surface, a modification of the surface with Poly-L-lysine was carried out.

Other samples were treated with a 0.5 % solution of NaOCl in water for at least half an hour [44]. The remaining solution was sucked away and a 1 M HCl solution was poured in the chamber. After half an hour the solution was again sucked away and the surface was rinsed twice with de-ionized water. The samples were sterilized as mentioned above under UV irradiation and cells were seeded.

Modifications with UV light of a wavelength of 172 nm which was also carried out in the above mentioned paper, were not tried.

3.2. Activation of ion channels in HEK cells

As stated in the introduction it should be possible to activate ion channels by polarizing the membrane with a polarized dielectric. To check if this is possible for organic dielectrics the following experiment was designed (Figure 36).

Cells are seeded above the dielectric covered metal electrodes and after one day of incubation they are transfected with calcium ion channels. By applying a bias between a bath electrode and the metal electrode under the dielectric, the dielectric will be polarized, leading to a polarization of the membrane, which then will open the ion channel. If this is the case, calcium ions stream into the cell and bind there to the Ca^{2+} selective fluorescence dye FURA-2AM (Figure 35, excitation wavelength $\lambda = 340$ nm & $\lambda = 380$ nm), which can be detected by fluorescence microscopy.

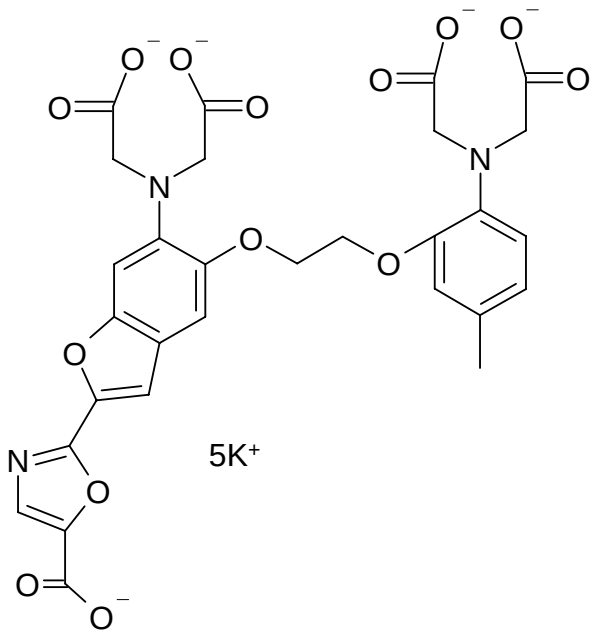

Figure 35: Fura-2AM molecule

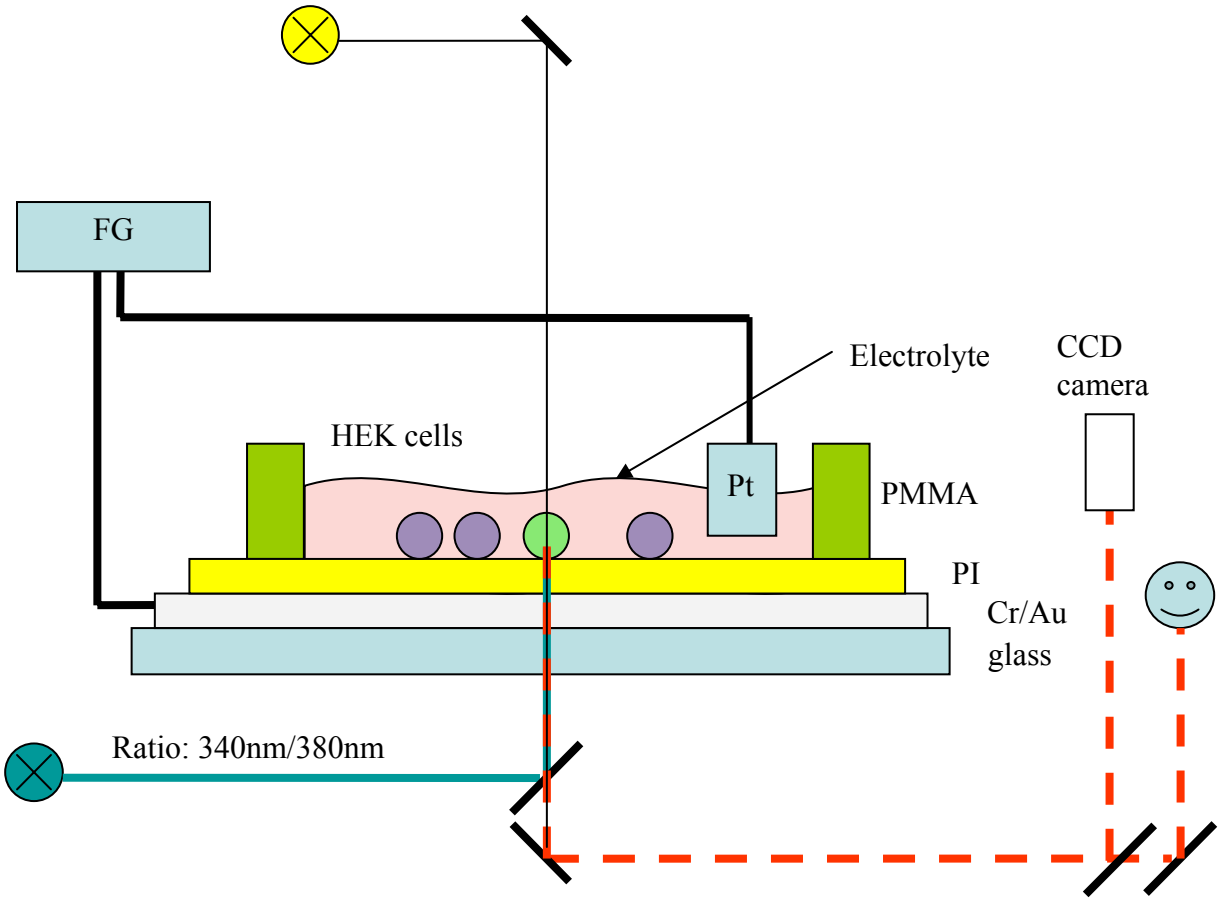

Figure 36: Ion channel activation experiment

3.2.1. Device Preparation

After cleaning glass cover slides metal electrodes were vacuum deposited. This was done with the evaporation unit inside glove box II. Because light microscopy should be carried out in the further course of the experiment the electrodes were design to be transparent. Therefore a 20 nm gold electrode was evaporated. To ensure adherence of the electrode to the glass surface a 1 nm chromium layer was first applied to the glass. Five samples were prepared with ZnO doped with Al sputtered onto cover glasses as an electrode.

Afterwards the dielectric was spun onto the slides and again removed from the edges of the electrodes to be able to contact them later. For this experiment the results of the cell compatibility test where applied so that only *Polyimide* was used. After the annealing step of PI at 180 °C a PMMA ring was glued to the PI-cover slide to contain the cell medium away from the electrodes. As glue the polyimide precursor was used after preliminary experiments showed that usual glues transpired remaining solvents into the cell medium leading to death of the cells.

With respect to the low glass temperature of PMMA (T_g = 110°C) the curing of the polyimide cursor was reduced to 150 – 160 °C. At this temperature the Polyimide precursor is not fully cross linked but with the deformation of the PMMA ring good enough to fix the ring to the PI layer and to seal the so formed cell compartment from the electrodes.

As usually sterilization was done overnight with UV irradiation. Experiments were usually started on Mondays with seeding the cells. The cells were incubated at 37 °C in CO_2 atmosphere overnight and checked with the light microscope on the next day. When on some days the cells did not adhere but formed clusters, the planned transfection of the cells with the ion channel was postponed because not adhering cells are exposed to a high level of stress and their metabolism changes completely so they are not going to express the ion channel in their membrane.

3.2.2. Dielectric check

To ensure that no electrochemical reactions will take place when a current is running through the electrodes the dielectric above should be pin hole free. To check this, the samples were filled with 1 ml saturated sodium chloride solution and a Pt electrode was put into the bath. Between the two electrodes the Impedance and the angle θ (as explained above in 2.3.2) was measured at 10 and 100 kHz. When the angle θ is close to -90° the material is considered as not conducting, whereas angles close to zero are a sign for pin holes or that the material is a conductor.

3.2.3. Transfection

Transfection describes the transfer of DNA inside a cell [45], which then will be expressed inside forming for example an ion channel. (Figure 37)

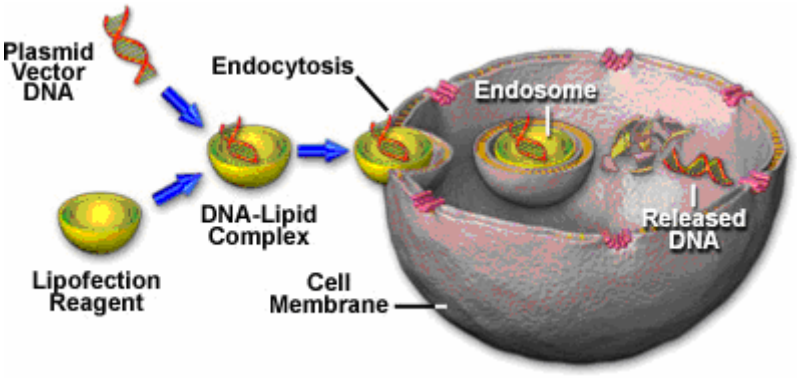

Figure 37:Lipid-mediated transfection in mammalian cells (taken from [46])

In general two kinds of transfection exist: *transient* and *stable* transfection.

By *transient* transfection is meant that the DNA is not added to the host genome but is extra chromosomal inside the Plasmid and is transported to the cell core for transcription. Since the DNA is not in the cell core it is not handed to the next generation.
Stable transfection is meant when the inserted DNA is taken up into the host genome and can therefore be handed to the next cell generation. Compared to the transient transfection which can be applied easily for most of the cell lines and different kinds of DNA it takes some time to get a stable transfected cell line. However when a stable cell line is achieved, one gets always the same clones, which can be used for a long time until the gene is expelled from the core again. [47]
In general six different techniques are available:

- Calciumphosphat-Coprecipitation
- Elektroporation
- Lipofection
- Nanofectin™ (PAA)
- Mikroinjection
- DEAE-Dextran-Method

In the course of this thesis *transient* transfections by Lipofection were carried out. Different transfection agents were used to check which one will give the highest yield of transfected cells, which depends on the combination of cell line type and DNA:

- Transfectin™ Lipid Reagent by *BIO-RAD*
- Superfect™ by *Quiagen*
- ExGen500™ by *Fermentas*
- Lipofectamin™ by *Invitrogen*

The transfection protocols can be found in the Appendix B.
Figure 38 shows a successful transfection of HEK293 cells with ExGen500 with an estimated transfection efficiency of ~80% according to the manufacturer [48].

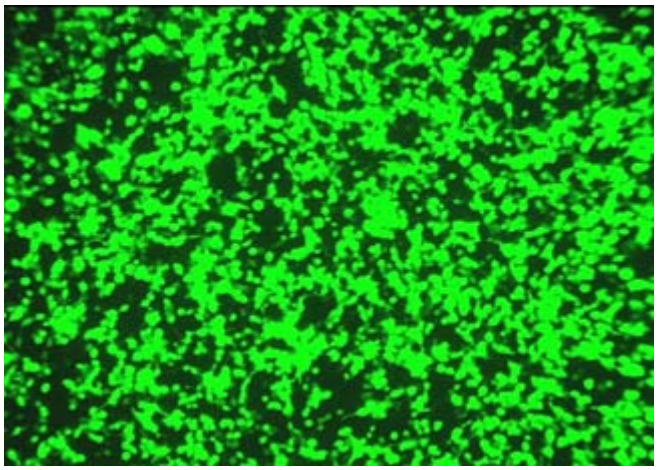

Figure 38: Successfully transfected HEK293 cells (taken from [48])

The ion channel that should be expressed by the cell in the plasma membrane consists of three proteins described by three DNA plasmids: the α1c plasmid, the β2α plasmid and the α2δ plasmid. The α1c subunit is also encoded with the fluorescence marker EYFP (enhanced yellow fluorescence protein, excitation wavelength λ = 513 nm), so that the success of the transfection can be monitored also by fluorescence microscopy.

3.2.4. Imaging

Transmitted light and fluorescence microscopy was carried out on the Zeiss Axiovert135 microscope (Figure 39) equipped with a SensiCam CCD Camera.

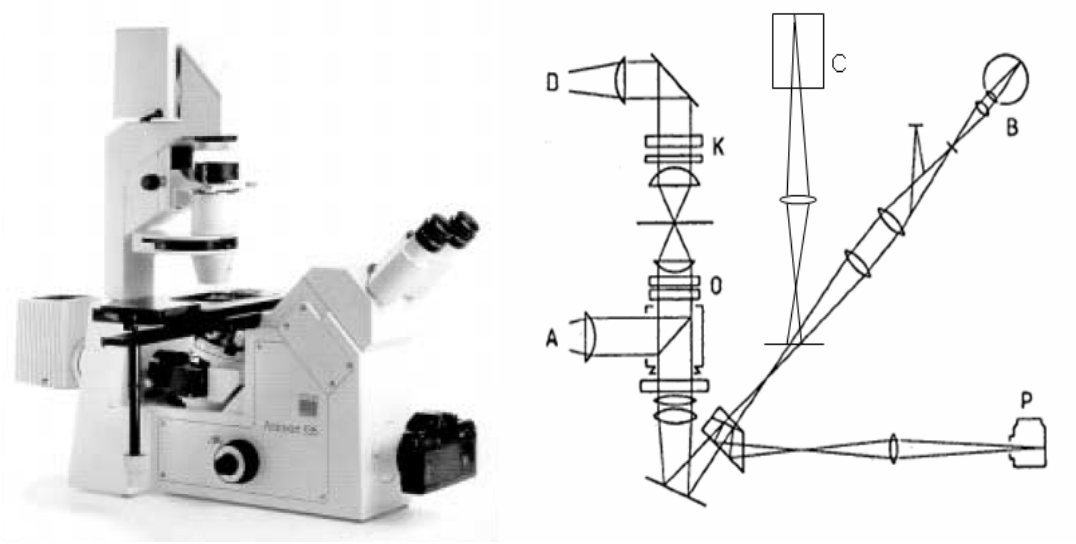

Figure 39: Inverted microscope Axiovert 135 by Zeiss

(D) Transmitted Light, (A) Reflected Light (fluorescence light source), (B) Observation beam path, (C) CCD Camera, (P) Photo beam path (not used in our case), (K) Condenser, (O) Objective & Filter block

3.3. Impedance measurements

To see if a tight adhering cell layer changes the capacitance or the impedance of the dielectric layer impedance measurements were carried out. Since the electrodes cannot be put onto the cell layer the measurements were carried out with a platinum electrode in the cell medium as a second electrode (same measurement setup as seen in Figure 36).
The same samples produced for the above mentioned experiment were also used for Impedance measurements. The frequency dependent impedance was measured using a HP4284A Precision LCR meter (frequency range: 20 Hz – 1MHz).

3.4. Capacitance Measurement

Capacitance measurements with metal-insulator-metal (MIM) devices were made to compare the resulting capacitance per unit area with values used in cell – chip junction experiments. The measurement was carried out with the above mentioned HP4284A Precision LCR meter (frequency range: 20 Hz – 1MHz).

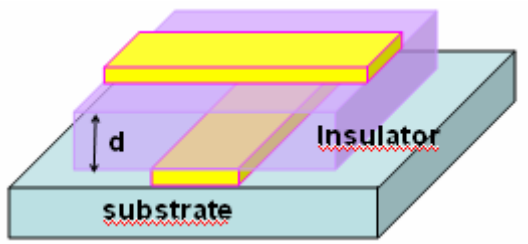

Figure 40: MIM-Device

Usually the used ITO glass was etched using HCl_{conz} and cleaned afterwards with Hellmanex and rinsed with water. The dielectric was deposited by spin coating and as a second electrode aluminium was used.
The samples used for the Impedance vs. Frequency measurements were also used to measure capacitance to check if adhering cells onto the surface have an influence.

3.5. I-V Measurements

Similar to the Impedance – Frequency measurements for dielectrics, Current – Voltage (I-V) measurements were carried out for the cells on semiconductor materials. Measurement was made with the AGILENT E5273A 2 channel source/monitor unit using just one output channel.

3.6. Top gate transistor

To activate a transistor with a cell as a gate, the operating gate voltage of the transistor has to be rather low, because the voltage change that can be achieved by the opening of a ion channel is in the order of some 10 mV. After studying the literature a suitable candidate was found in a transistor consisting of P3HT as active material and PEO:$LiClO_4$ as a polyelectrolyte dielectric was used [51]. After discovering that PEO is water-soluble further experiments to improve the transistor were cancelled.
Employing the results of the cell compatibility tests top gate transistors (Figure 24) with the suitable dielectrics, were built to show that they are also capable to make good top gate transistors. Therefore polyimide and cross linked polyvinylphenol were chosen as gate dielectric.

3.6.1. Device preparation

To get this device 1.5 cm x 1.5 cm glass slides were thoroughly washed with Hellmanex cleaning solution in the warm ultrasonic bath for at least 15 minutes before rinsing them with de-ionized water twice and dried with pressurized air.
60 nm aluminum source drain electrodes were evaporated using a shadow mask in the evaporation machine inside the glove box. Afterwards the samples were transferred to the UNIVEX350 evaporation machine for C_{60} evaporation. C_{60} was chosen as active material because it is supposed to withstand the elevated temperatures needed to thermally cross link the Polyimide and Polyvinylphenol precursors.
Usually 200 nm of C_{60} were evaporated at an average speed of 0.7 Å/sec and a base pressure of ~5.0 x 10^{-6} mbar in the UNIVEX350 evaporation machine.

After transferring the samples back into the glove box I, they were spin coated with the precursor solution with the standard spin coating program: in 4 seconds to 1500 rpm, stay there for 40, accelerate to 2000 within one second and keep the speed for 20 seconds before reducing the speed again.
Unfortunately the solvents used in the precursor solution N-methylpyrrolidon (NMP) for polyimide and Propyleneglycolmonomethyletheracetat (PMA) for cross linked PVP were very aggressive towards the deposited C_{60} layer. A drop of NMP strips a 200 nm C_{60} film of the glass within a few minutes. During spin coating this effect can also be observed causing inhomogeneous films, which results in not working devices.
Polyimide samples were cured on the hot plate, first at 75 °C for 30 minutes to avoid strong shrinking of the film, before heating to 180 °C for one hour as advised by the manufacturer. Polyvinylphenol samples were thermally annealed at 190 °C for 30 minutes using an oven.
Last but not least 40 nm aluminum were evaporated as gate electrode before testing the transistor using an AGILENT E5273A 2 channel source/monitor unit.

In another effort, not directly related to the cell-chip junction, a top gate transistor based on P3HT was build. As a gate dielectric Polyethyleneoxide (PEO) with $LiClO_4$, a solid electrolyte, was used.

As a substrate 1.5 x 1.5 cm glass slides were used, clean in Hellmanex glass cleaning solution and rinsed with water. Afterwards P3HT was spin coated from a 3 % solution in Chlorobenzene with the standard spin coating program inside the glove box.
After the semiconductor layer had dried, 40 nm gold source & drain electrodes were evaporated. The PEO:$LiClO_4$ electrolyte solution was drop casted outside the glovebox. On the next day, 40 nm gold were evaporated to form the gate electrode. Measurement was carried out inside the glove box.

4. Results and Discussion:

4.1. Results of Compatibility test

In the following section the results from the compatibility study of cell and dielectric/semiconductor surface are shown.

First, as comparison a picture of cells on glass (the confluence, the percentage of capacity of a cell culture medium used by cells is around 80 %) is shown in Figure 41: after 24 hours of cultivation, they show typical epithelial – like morphology and a typical length of about 40 – 80 µm.

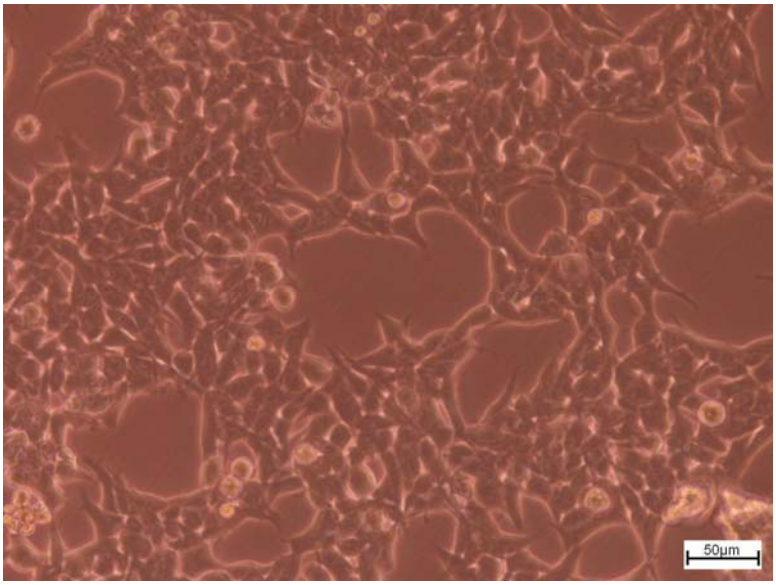

Figure 41: A typical microscopic image of HEK293 cells on glass slides

Note: In general the color of the pictures does not only show the color of the material which was spin coated or evaporated onto the cover slides but also depends on the age of the sample. One of the ingredients of the DMEM is Phenol Red, a pH-indicator, which changes its color more to yellow the more acid the solution is. The pH of the solution changes because the cells give their waste products to the solution.

4.1.1. Dielectrics

Benzocyclobutadiene (BCB): The picture of HEK293 cells cultivated on untreated BCB (Figure 42) shows that the cells are not adhering to the surface, most likely because BCB is highly hydrophobic and therefore not very suitable for the cells. Not adhering HEK cells tend to form clusters to reduce their surface and therefore their vulnerability.

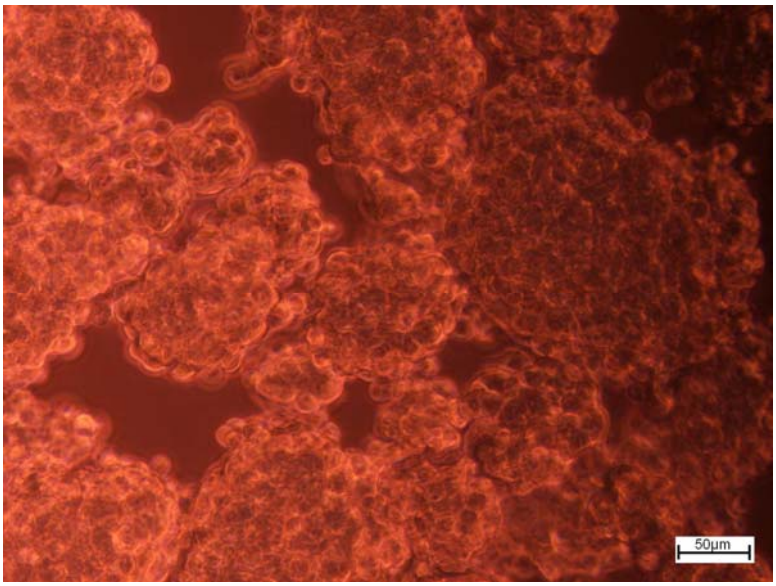

Figure 42: Cell clustering on top of untreated BCB

To increase adhering of the cells to the BCB surface it was treated with 0.5 % NaClO solution as mentioned above to decrease the hydrophobic character of the surface. The NaClO solution didn't wet the surface completely due to high surface energy and therefore the cell adherence after the treatment didn't differ very much. After three days the cluster has sunk down and some of the cells were forced to adhere (Figure 43). Nevertheless these samples couldn't be used for any further experiments because as soon as the sample was carried around or shaken a little the cells displaced and the clusters were floating again.

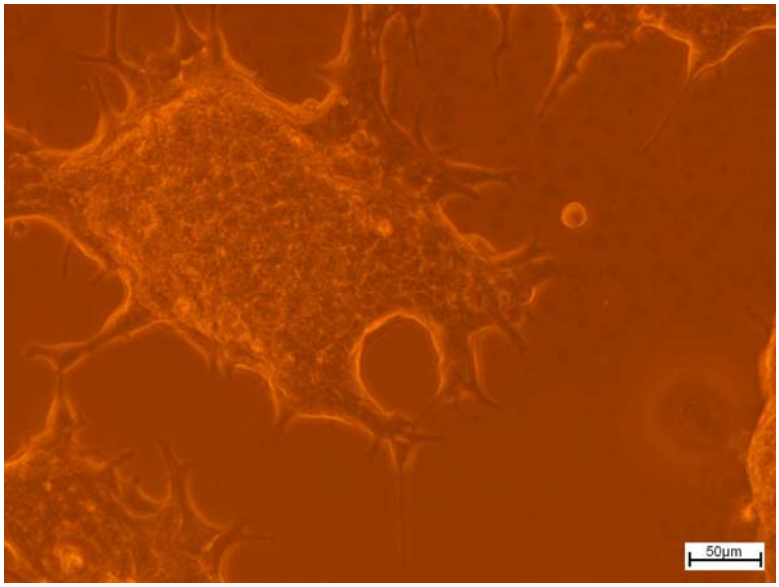

Figure 43: Slightly adhering cell cluster on treated BCB glass cover slide

Polyimide (PI): HEK293 cells on polyimide (Figure 44) show a similar behavior as the cells seeded on glass but the confluence of cells is much lower than on glass (~ 30 %).

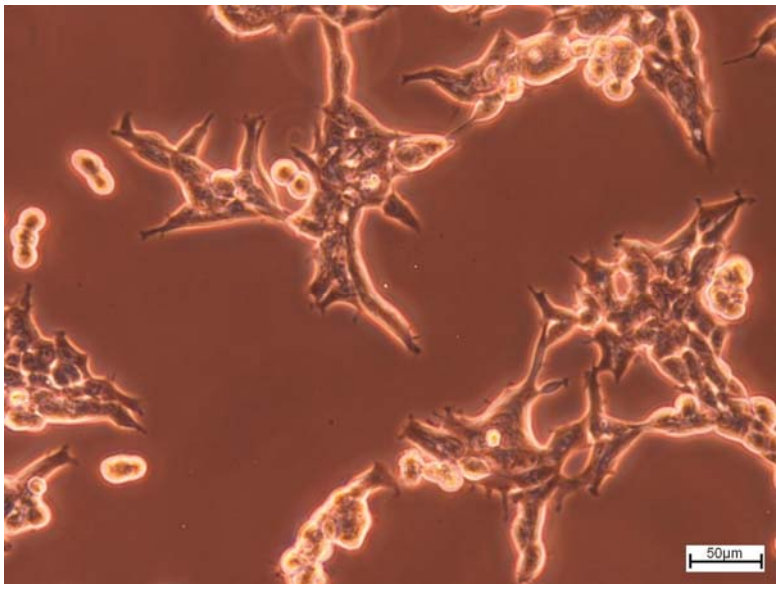

Figure 44: HEK293 cells on untreated polyimide

Therefore the polyimide surface was also treated with NaOCl prior to cell seeding and the confluence increased drastically leaving nearly no empty spots. Note the shadow in the middle of the picture is the Cr/Au electrode under the polyimide surface (Figure 45).

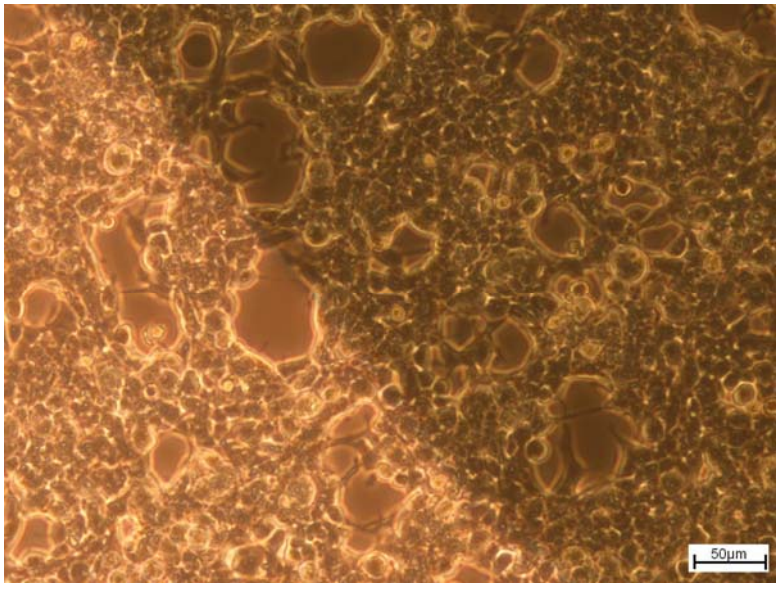

Figure 45: Cells on NaOCl treated polyimide with semitransparent Cr/Au electrode (dark area)

It is worth mentioning here that the experiments showed that the cells detach after four to five days very easily again from the surface due to very high confluence (~100 %). At this point some of the cells grow in a second layer and they are more susceptible to detaching and then they carry away lots of other cells.

Crosslinked Polyvinylphenol (PVP_{xl}): Very similar to polyimide, the cells adhere to PVP_{xl} only in a low confluence (~ 30 %) as can be seen in Figure 46:

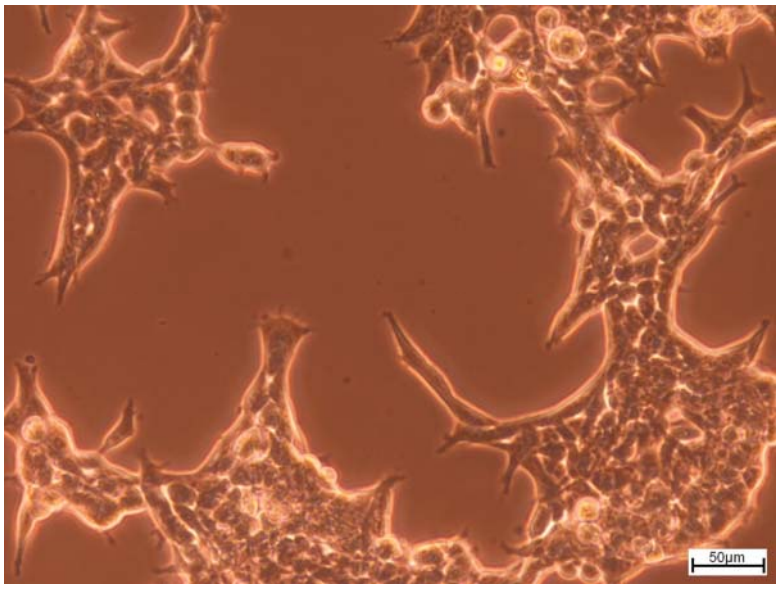

Figure 46: HEK293 cells on untreated PVP_{xl}

After treatment with NaClO more cells (confluence ~ 70 %) adhere to the surface as can be seen below (Figure 47). Also in the caseo of PVP_{xl} the cells start growing in a second layer and start to detach fro the surface.

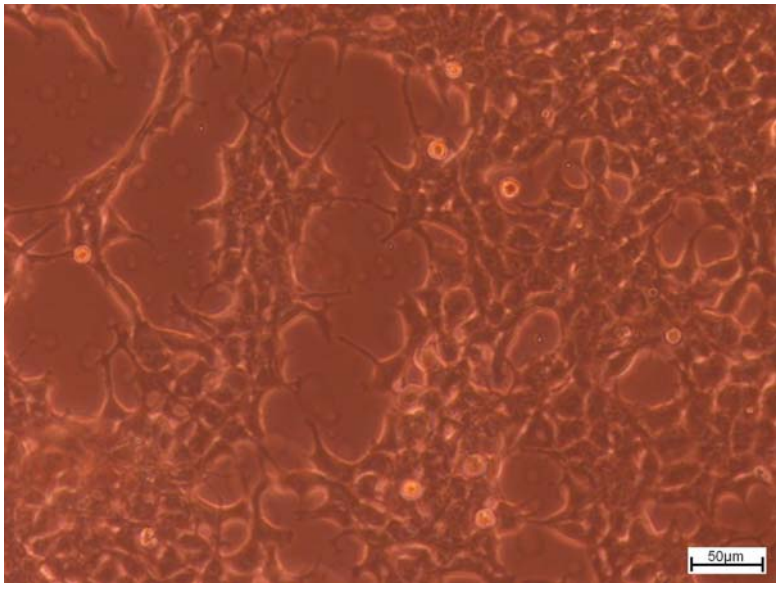

Figure 47: HEK293 cells on NaClO treated PVP_{xl}

Polymethylmethacrylat (PMMA): HEK293 cells grow very confluent (~ 70 %) on PMMA as can be seen in Figure 48, but the PMMA film starts to swell in aqueous media, what makes it unsuitable for electrical interfaces.

In the case of PMMA treatment with NaClO doesn't lead to a higher confluence as can be seen in Figure 49. Another reason for not using PMMA for further experiments besides

swelling of the material was that the time till the cells detached is rather short. After three days the cells start to grow above each other which makes them more susceptible to detaching. (Figure 49 upper right corner)

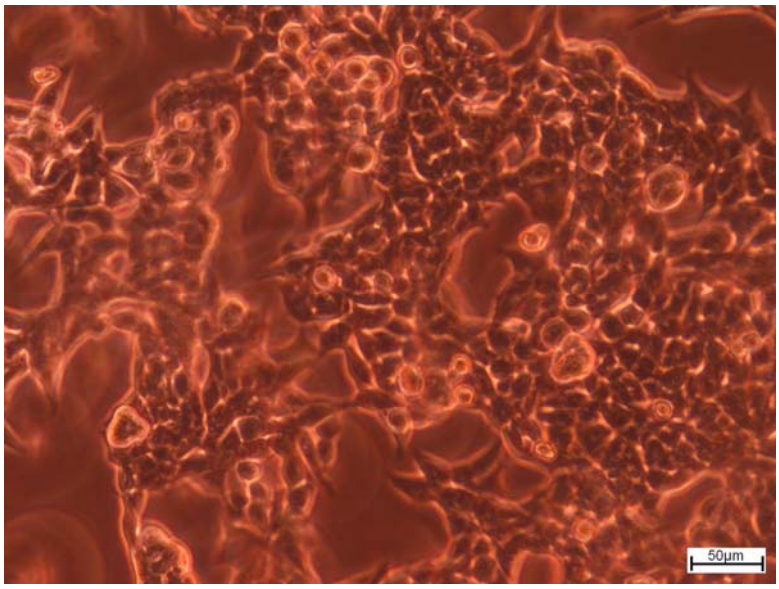

Figure 48: HEK293 on untreated PMMA

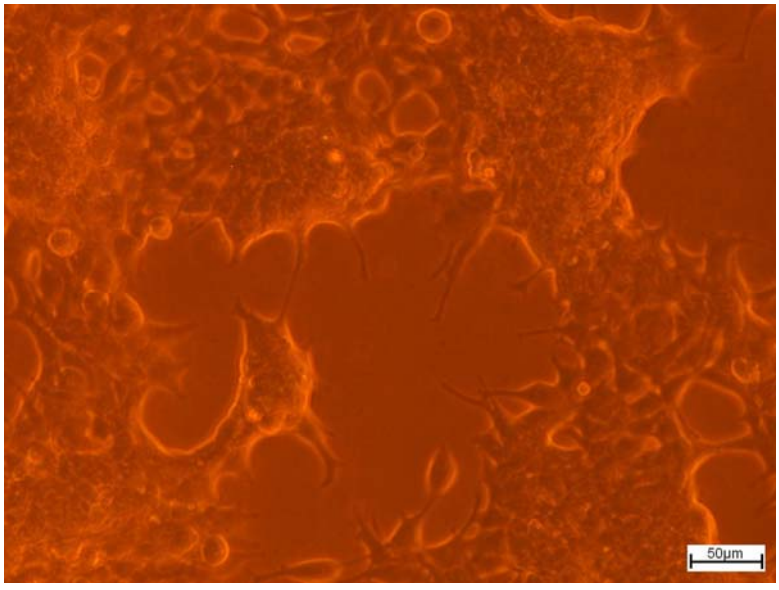

Figure 49: HEK293 on NaClO treated PMMA, day 3 after seeding

DNA – CTMA:

Samples with spin coated DNA-CTMA complex were always a problem. On the one hand some samples showed typical signs of contaminated surfaces as can be seen in Figure 50 although they had been fabricated parallel to other samples, which didn't show any sign of contamination.

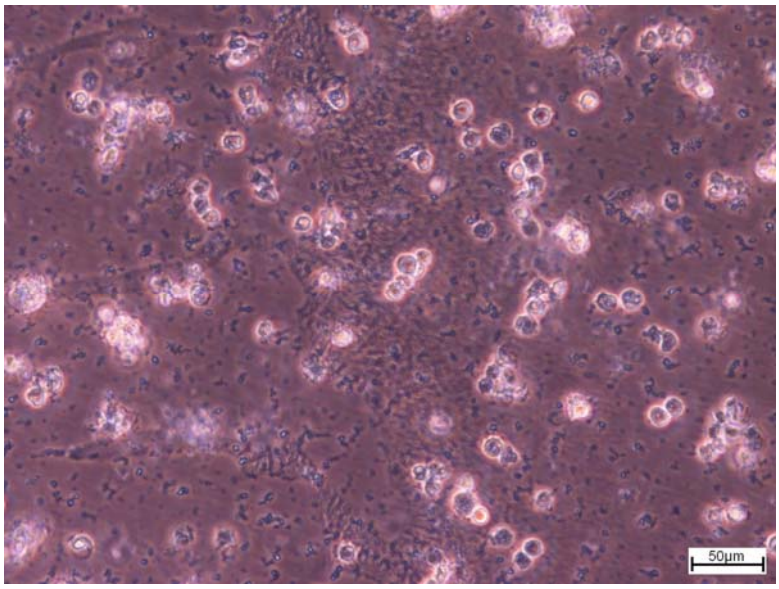

Figure 50: Maybe contaminated HEK29 cell culture on DNA-CTMA

On the other hand some very regular structures could be observed on the surface (Figure 51) and to the best of our knowledge, these structures does not posses HEK cells. Further test what these structures are and where they come from have to be investigated in further studies.

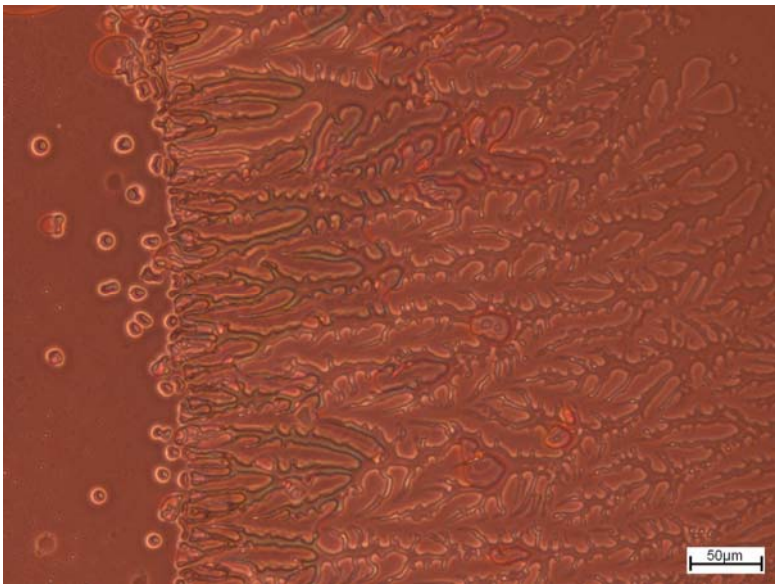

Figure 51: Regular structures in DNA-CTMA based HEK293 cell culure

Cyanoethylpullulan (CyEPl): HEK293 cells cultured onto CyEPl covered microscopy glasses were repelled by the surface similar to BCB as can be seen in Figure 52 and formed small floating clusters.

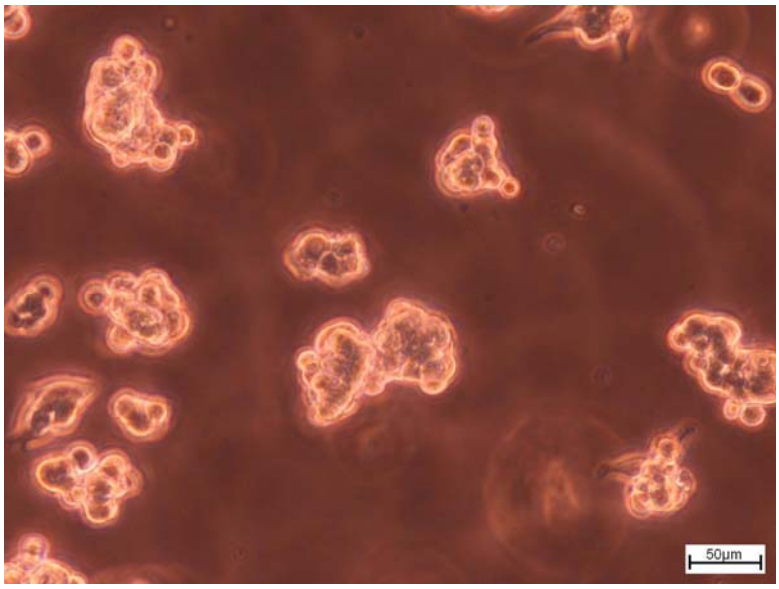

Figure 52: floating HEK293 cell clusters on CyEPl

Polystyrene (PS): On PS coated surfaces no adhering HEK293 cells could be observed. Additionally the PS surface is very brittle and has a lot of cracks as can be seen in Figure 53. The unfocused shadows on the left and right corners are floating cell clusters.

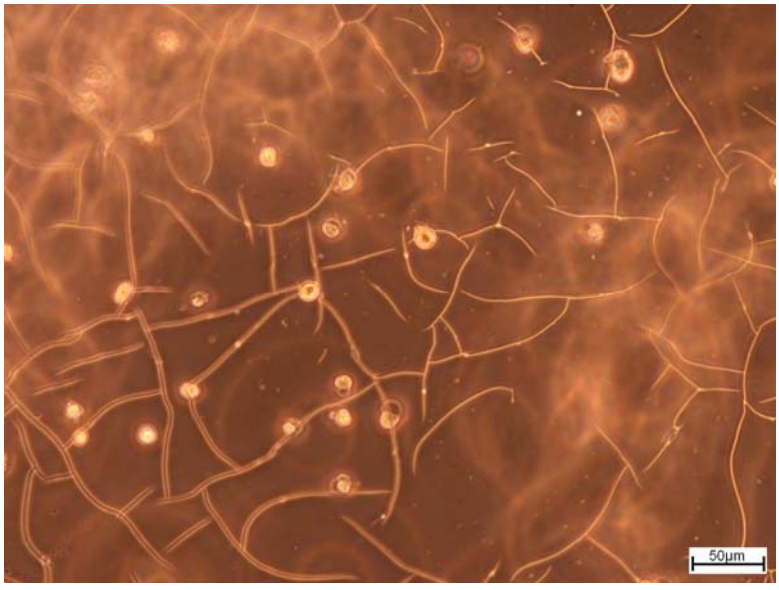

Figure 53: Cracks on PS surface

Sylgard184®: The HEK293 cells cultured on the two component silicone elastomer didn't adhere to the highly hydrophobic surface at all but formed floating cells clusters as can be seen in Figure 54.

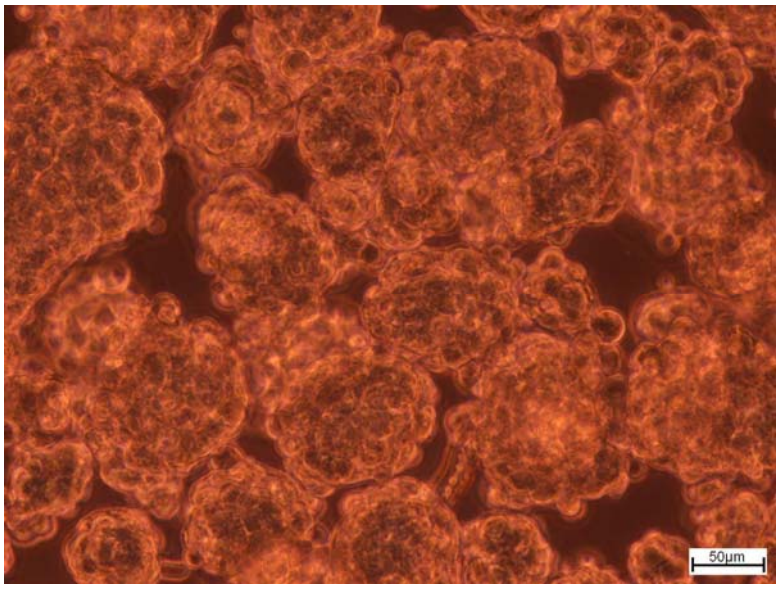

Figure 54: HEK293 cell clusters on Sylgard® elastomer

4.1.2. Semiconductor materials

Pentacene: As can be seen on Figure 55 the HEK293 cells didn't adhere to the evaporated Pentacene film, which is highly hydrophobic. Only on spots were the glass was not covered by the pentacene some cells adhere and other cells attach to these cells.

Figure 55: HEK293 cell cultured on Pentacene

Another problem with Pentacene is that the film itself is peeled off the glass substrate in the aqueous media (Figure 56), which might be different when using a metal electrode under the pentacene.

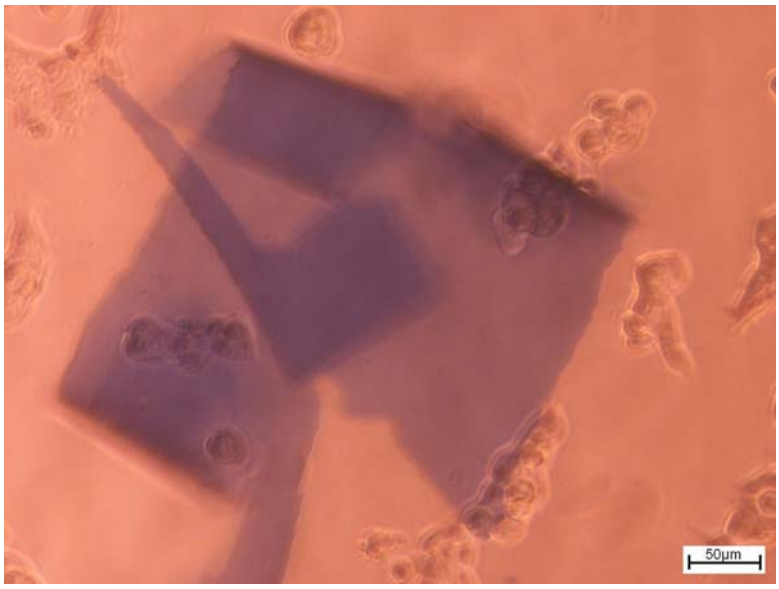

Figure 56: Detached Pentacene film on glass

Poly-(3-hexylthiophene-2, 5-diyl (P3HT)): HEK293 cells form clusters on the P3HT film (Figure 57), spin coated from chlorobenzene solution. Remarkable is that there seems to be no more toxic chlorobenzene in the film which could harm the cells.

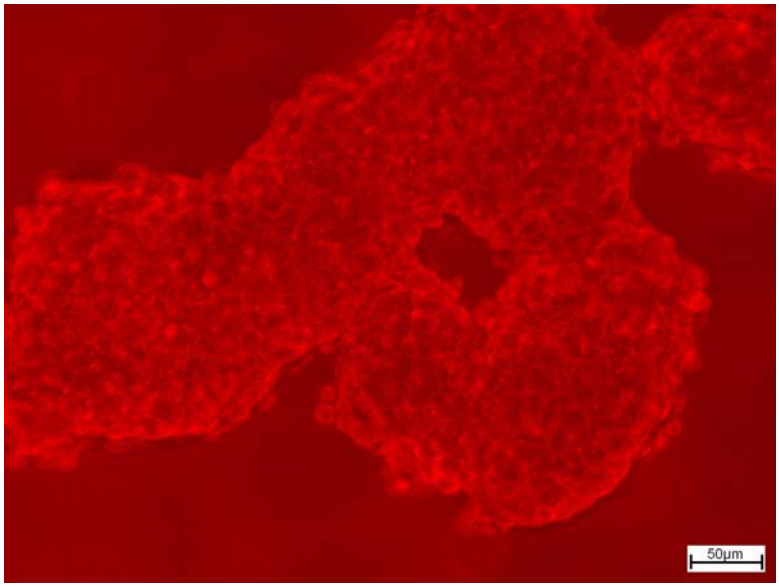

Figure 57: HEK cell cluster floating above P3HT

C_{60}: Very similar to pentacene the HEK293 cells do not adhere to the evaporated C_{60} film but form clusters instead (Figure 58). Positively is that the C_{60} film still adheres to glass upon exposure to the aqueous media.

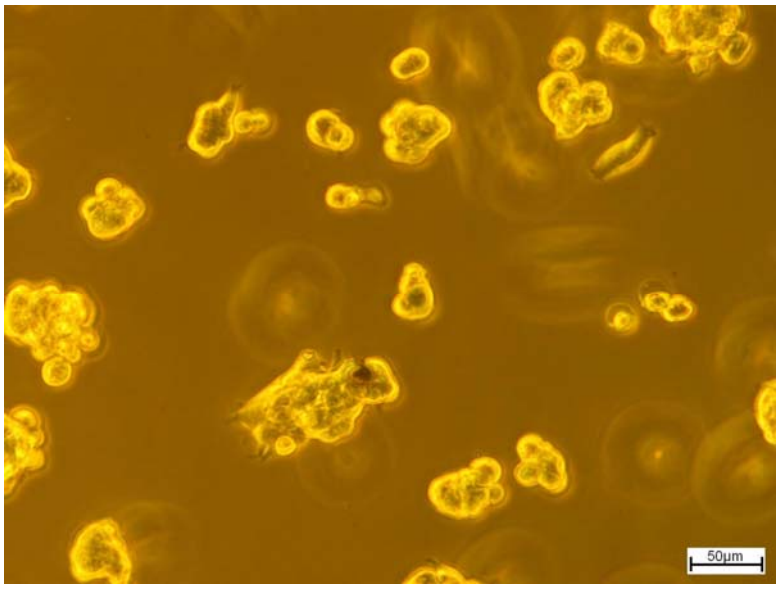

Figure 58: HEK cell clusters on C_{60}

ZnPc:

Like in the cases above the cells also do not adhere very well to Zinc Phthalocyanine but form clusters instead (Figure 59).

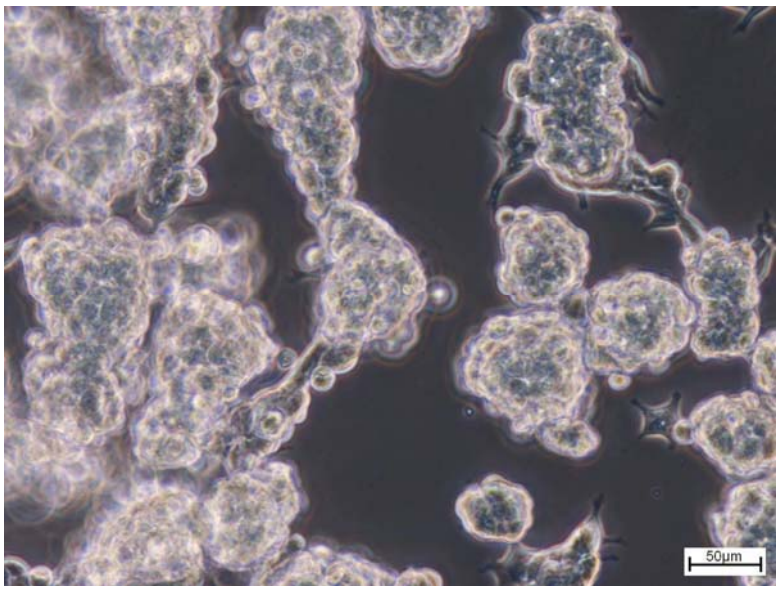

Figure 59: HEK cells on ZnPc

4.2. Activation of ion channels in HEK293 cells

4.2.1. Transfection results

The success of the transfection of the HEK293 cells with the L-type Ca^{2+}-channel was monitored with normal light (left-hand side) and fluorescence light microscopy (right-hand side). Since the Ca^{2+} channel is located in the membrane and it is labeled with an enhanced yellow fluorescence protein (YFP), it can easily be observed by fluorescence microscopy under 513 nm light excitation.

Pictures below show successful transfection for all transfection reagents (bright spots in right-hand figures below) but the yield of transfected cells is generally quite low (larged dark areas).

The best transfection reagent for this combination of cell line and DNA seems to be the Transfection™ Lipid Reagent by BIO-RAD because the cells remain attached to the dielectric surface (Figure 60 left).

4.2.1.1. Transfectin™ Lipid Reagent by BIO-RAD

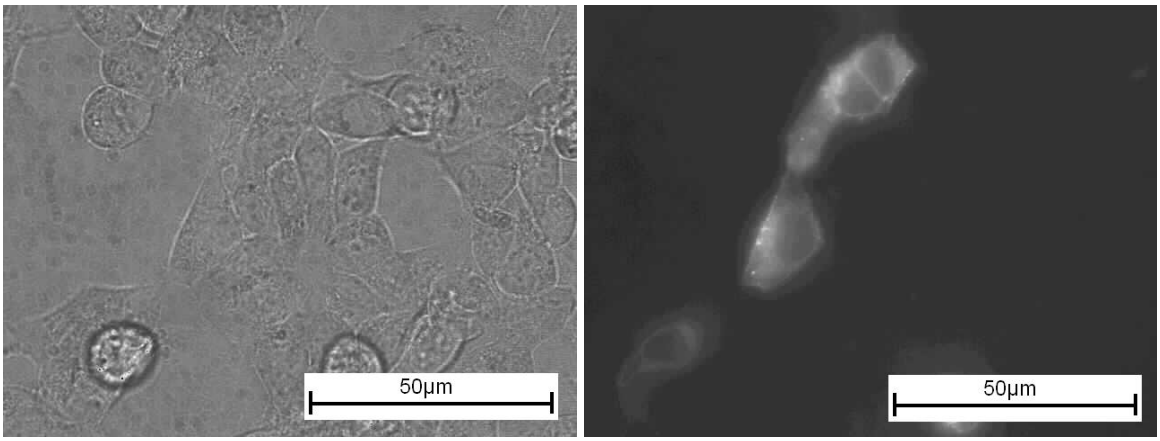

Figure 60: Transfection with Transfectin™: successfully transfected (right-hand side) cells with low yield but cells stay attached to the surface (left-hand side)

4.2.1.2. Superfect™ by Quiagen

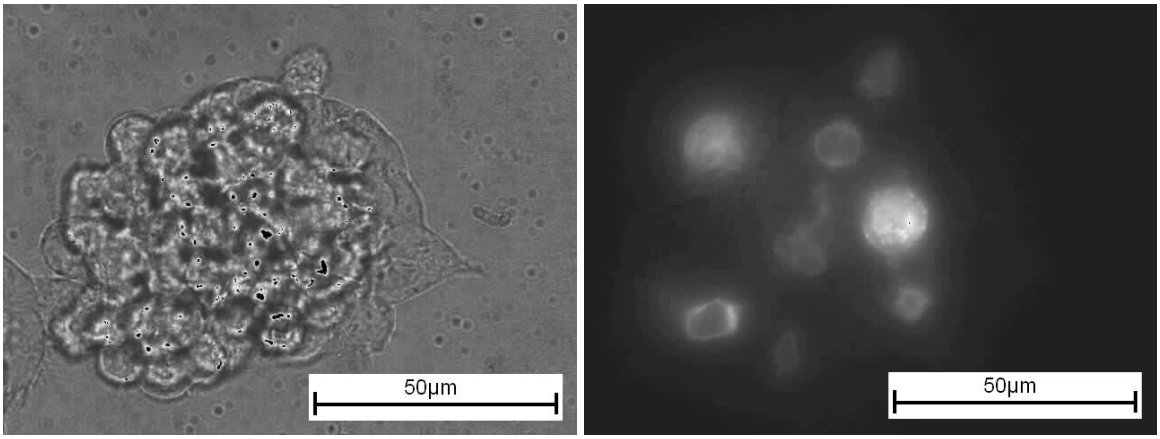

Figure 61: Transfection with Superfect™: successfully transfected (right-hand side) cells which detach from the surface and form clusters (left-hand side)

4.2.1.3. ExGen500™ by Fermentas

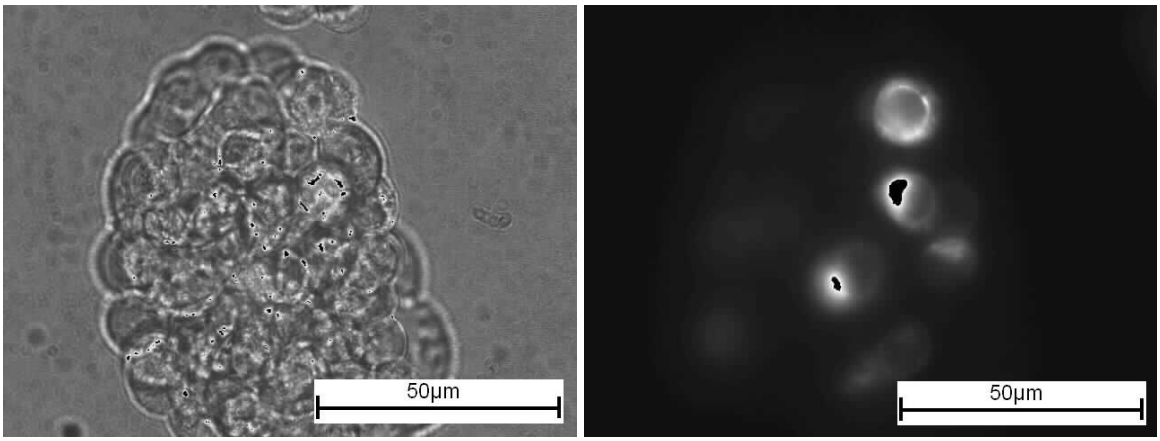

Figure 62: Transfection with ExGen500™: successfully transfected (right-hand side) cells which detach from the surface and form clusters (left-hand side)

4.2.1.4. Lipofectamin™ by Invitrogen

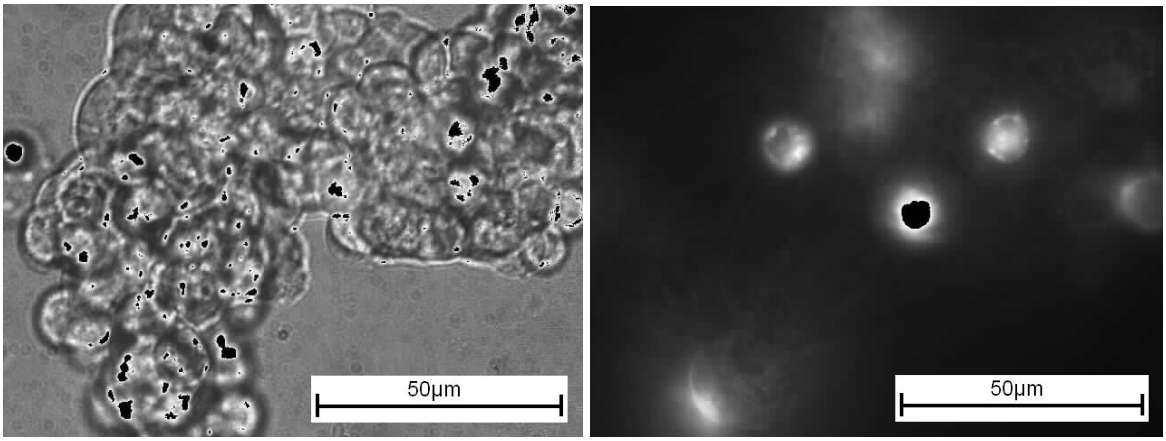

Figure 63: Transfection with Lipofectamin™: successfully transfected (right-hand side) cells which detach from the surface and form clusters (left-hand side)

Since the electrodes have a rather large area (~80 mm²) and therefore a large number of cells will be attached to the dielectric above, it will be very difficult to find exactly those cells which have been transfected successfully with ion channels. With a larger transfection yield the probability to find and observe the right cells would be increased.
The Transfection efficiency is heavily influenced by a various number of different parameters like the used cell line, the serum, the used vector, the DNA and also the stress level of the cell culture itself. [50].
Beside the problem of a low transfection yield, another problem occurred during fluorescence microscopy with the metal electrode covered glass slides. Due to the microscopy geometry all light was reflected by the metal electrode. This means that no signal from cells sitting above the electrode can be seen due to this high intensity of the reflected light.

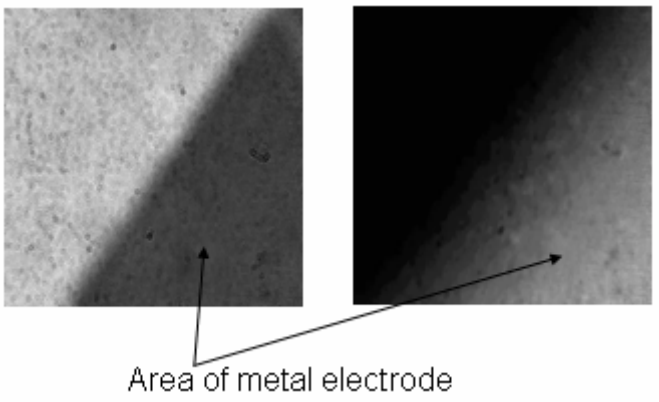

Figure 64: Electrode under direkt light (left) and under fluourescence light

The light area in the right picture is in reality green, the color of the incident fluorescent light, but unfortunately the CCD camera can't give true color pictures.

The same problem was observed with Indium-Tin-Oxide (ITO) covered glass but sputtered Zincoxide (ZnO) doped with aluminum showed high transparency for the fluorescence light. Unfortunately only five of these samples were available so that the experiment cannot be continued at this time.

4.3. Impedance measurements

Cells were seeded on a polyimide covered glass slide with Cr/Au metal electrode and incubated for 24 hours. Impedance versus frequency measurement was carried out using a Pt counter electrode. The following graph shows recorded curves with and without cells. As can be seen in Figure 65 the sample with the cells has a remarkable higher Impedance Z compared to the sample without. The measurement was carried out between 1 kHz and 1 MHz and gave the following results:

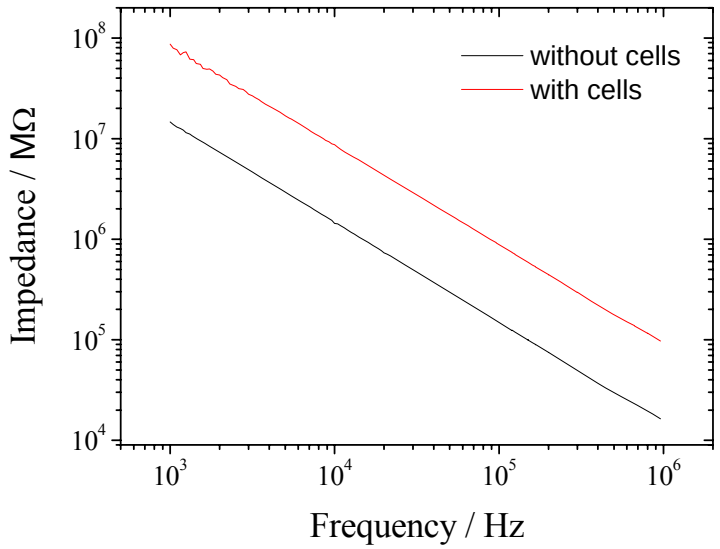

Figure 65: Impedance vs. frequency measurement for sample with and without cells

As expected the impedance goes linearly down with frequency in the double logarithmic plot, but the big difference in impedance cannot be assured to the presence of cells onto the surface, but can also origin in a different thickness of dielectric. Also it is very problematic to say that a certain value refers to a certain number of cells because it is hard to quantify them when they are attached to the surface.

4.4. Capacitance Measurement

4.4.1. MIM results

The following table lists the results of the MIM device capacitance measurements.

Table 1 Capacitance per unit area of selected organic dielectrics

Material	Capacitance per unit area (nF/cm^2)	Layer thickness (nm)	Dielectric constant
BCB	1.2	2000	2.7
BCB (1:1)*	4	600	2.7
PI	2.0	1500	3.4
PVP_{xl}	10.5	500	5
PMMA	6.4	500	3.6
DNA-CTMA	6.9	1000	7.7
CyEPl	10.6	1000	12
PS	2.25	1200	2.55
PDMS	0.78	3000	2.65

*… diluted with Mesitylene by volume

As one can see from the table above the values for capacitance per unit area are far below the value of a cell membrane ($1\mu F/cm^2$). This is due to the large thickness of the films which are orders of magnitude thicker than the SiO_2 films used by the Fromherz group.

The thicknesses above are achieved by standard spin coating program and may be reduced by elevated spinner speed or by more diluted precursor solutions. But there seems to be a limit especially for thermally cured films which form pin holes when using very diluted solutions (e.g.: BCB : Mesitylene = 1:2) and in this case a bad dielectric layer is formed.

Using such samples for ion channel activation experiments is not a good idea as they would be short cut upon applying a voltage and electrochemistry would occur.

4.4.2. Capacitance measurement under cell influence

According to the measurement results the presence of adhering cells onto the dielectric seems to decrease the capacitance by a factor of 5. Since comparative measurements with and without cells were not carried out with the same sample there is an uncertainty in quantitative comparisons. However, the small thickness variations of the dielectric layers spin coated from the same solution and with the same program are not expected to be responsible for this effect by a factor of five which can be observed in the capacitance values. It is more likely that the effect is a result of a heavily increased thickness due to the additional cell layer (cell high assumed to be some µm).

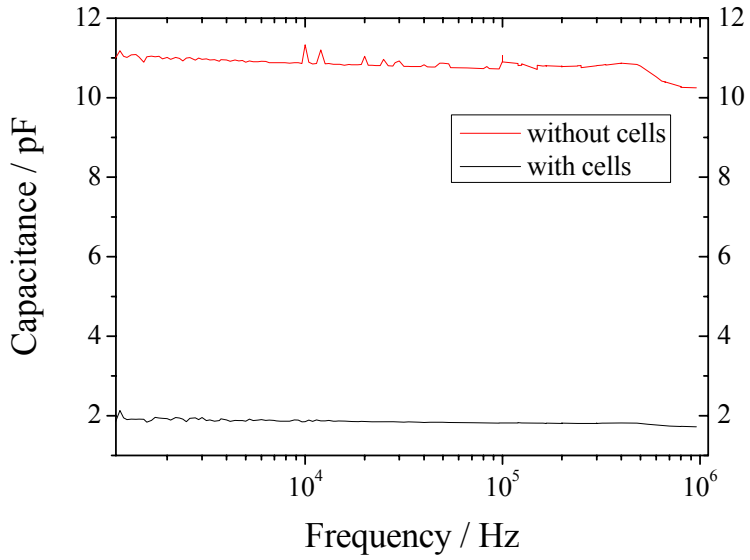

Figure 66: Capacitance change under the influence of cells adhering to the dielectric surface

4.5. Top gate transistor

The top gate transistor was characterized using the Agilent 2 Channel (high power / medium power) source monitor unit E5273A inside the glove box.

As mentioned above the top gate transistors based on C_{60} and PI and PVP_{xl} as a gate dielectric didn't work because the C_{60} was severely damaged by the aggressive solvents of PI and PVP_{xl} precursor solutions. This resulted in a bad transfer characteristic as can be seen in Figure 67

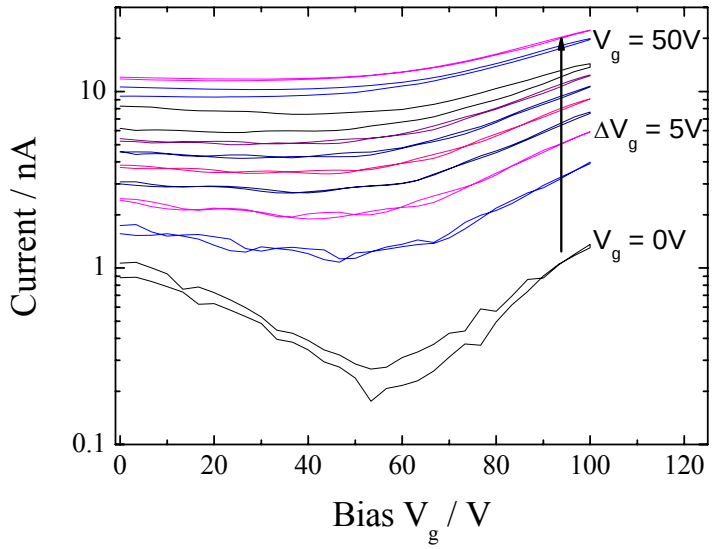

Figure 67: Transfer characteristic of top gate C_{60}/PI OFET

As mentioned above a top contact, top gate transistor based on P3HT and with PEO:$LiClO_4$ as a gate dielectric was produced. The following two graphs show the output characteristics (Figure 68) as well as the transfer characteristics (Figure 69) of the device.

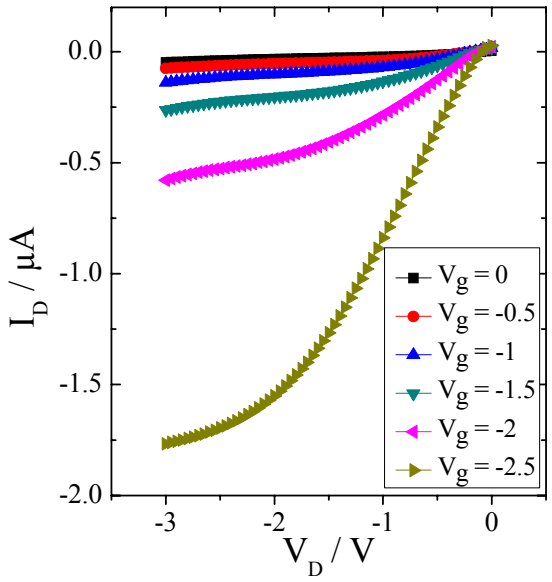

Figure 68: Output characteristics of top gate P3HT/PEO:$LiClO_4$ OFET

As can be seen in Figure 68, an hole accumulation mode is achieved with a negative bias gate voltage, V_g, demonstrating a p-type transistor behaviour.

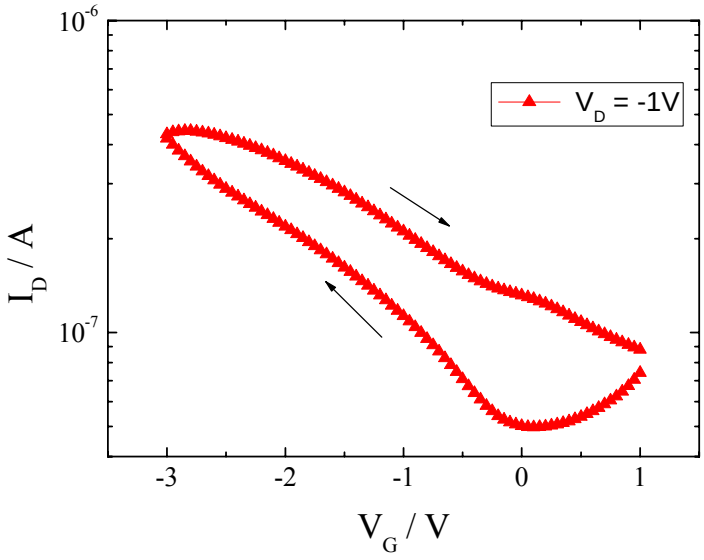

Figure 69: Transfer characteristic of top gate P3HT/PEO:$LiClO_4$ OFET

Following the forward curve from +1 to -3 V the transistor turns "on" at 0 V and current increases for one order of magnitude. In the backward direction the current stays higher over the whole scan area. This can be attributed to the mobile ions being trapped in the channel area which keep the channel between source and drain open [51]. This effect is called

hysteresis and forms bistable states, which can be used as a memory element if they do not decay to fast. If the transistor is not used as a memory device the hysteresis is considered to be parasitic.

The low turn on voltage is also a result of the mobile ions within the dielectric increasing the capacitance to ~5 μ/cm^2 [52]. This high capacitance would be perfect for cell chip junctions but unfortunately the PEO:$LiClO_4$ dielectric is water soluble and therefore no cell cultures can be seeded onto the dielectric.

5. Conclusions

During the course of this thesis work, feasibility of organic dielectric/ organic semiconductor and cell adhering properties on this surfaces have been successfully investigated.

As shown in section 4.1 only on a few dielectrics the cells adhered so well that further experiments were possible. For the semiconductor materials tested in this thesis such behavior couldn't be observed.

Further investigations on surface treatment and surface functionalization have to be done to ensure a tight adherence of the HEK cell culture to the dielectric. It is to be noted that different cell cultures behave different on various surfaces and that other cell cultures might form a better cell organic interface and hence be more suitable for this kind of experiments. For example, neurons could be used although they have the disadvantage that the best way to obtain them is by dissecting them from living animals.

Another problem as mentioned above is that the fluorescence light is reflected by the metal electrodes under the dielectric layer and therefore prohibits the ion channel activation experiment could be avoided by changing the microscopy setup. When the excitation light comes from above not parallel to the camera beam the ion channel activation experiment should be possible.

To solve the problem of relative low capacitance of organic dielectric layers, experiments with self assembled monolayers show promising capacitances with thicknesses down to 2.5nm can be achieved [53], and also a cross linking of water soluble PEO-electrolyte dielectric has to be taken into consideration, since these layers seem to have high capacitances, due to their high ion content.

From all this studies discussed above, it is very clear that some of the organic dielectrics and their cell adhering properties are feasible to explore much more towards a bio – cell chip interface.

6. References

1. J. Malmivuo, R. Plonsey, *Bioelectromagnetism*, Oxford University Press, New York, 1995, online available at: http://butler.cc.tut.fi/~malmivuo/bem/bembook/00/ti.htm (09.10.06)
2. J. Bardeen, W.H. Braittain, *Phys. Rew.* **74**, 232 (1948)
3. W. Shockley, *Bell Syst. Tech. J.*, **28**, 435 (1949)
4. J. E. Lilienfeld: US Patents 1,745,175 (1930), 1,877,140 (1932) & 1,900,018, (1933)
5. http://nobelprize.org/nobel_prizes/physics/laureates/1956/index.html
6. D. Kahng M. M. Attala. *IRE Device Research Conference, Pittsburgh* 1960
7. O. P. Hamill, A. Marty, E. Neher, B. Sakmann, F. J. Sigworth, *Pflügers Arch.* **391**, 85 - 100 (1981)
8. P. Fromherz „Brain Online – the feasibility of a neuron silicon junction", 20th Winter Seminar on "Molecules, Information and Memory" Klosters 1985 http://www.biochem.mpg.de/mnphys/publications/85fro/85fro.pdf (10.10.06)
9. For a collection of references look at: http://www.biochem.mpg.de/mnphys/publications/publications-e.html (24.10.06)
10. H. Shirakawa, E.J. Louis, A.G. MacDiarmid, C.K. Chiang, and A.J. Heeger. *J. Chem. Soc. Chem. Comm.*, **16**, 578 – 580, (1977)
11. C.K. Chiang, C.R. Fincher Jr, Y.W. Park, A.J. Heeger, E.J. Louis, H. Shirakawa, S.C. Gau, and A.G. MacDiarmid. *Phys. Rev. Lett.*, **39**, 1098 – 1101, (1977)
12. C.K. Chiang, M.A. Druy, S.C. Gau, A.J. Heeger, E.J. Louis, A.G. Mac-Diarmid, Y.W. Park, and H. Shirakawa. *J. Am. Chem. Soc.*, **100**, 1013, (1978)
13. A. Heeger in: *Nobel Lectures, Chemistry 1996 - 2000*, Edited by: I. Grenthe, World Scientific Publishing Co., Singapore, 2003, 380 – 417 http://nobelprize.org/nobel_prizes/chemistry/laureates/2000/heeger-lecture.html (10.10.06)
14. Fromherz in: *Nanoelectronics and Information Technology,* chapter 32: Neuroelectronic Interfacing: Semiconductor Chips with Ion Channels, Nerve Cells and Brain. Edited by: R. Waser, Wiley-VCH, Berlin, 2003, 781 – 810
15. M. J. Schleiden, T. Schwann, M. Schulze, *Klassische Schriften der Zellenlehre*, Harry Deutsch Verlag, Frankfurt am Main, 2. Auflage, 2003
16. B. Alberts, D. Bray, A. Johnson, J. Lewis, M. Raff, K. Roberts, P. Walters: *Lehrbuch der molecularen Zellbiologie*, Wiley-VCH, Weinheim, 2001 2. überarbeitete Auflage

17. http://upload.wikimedia.org/wikipedia/de/8/80/Zelle_%28biologie%29.png (10.10.06)
18. http://upload.wikimedia.org/wikipedia/de/5/54/Doppellipidschicht.jpg (10.10.06)
19. M. F. Perutz in: Nobel Lectures, Chemistry 1942 – 1962, Elsevier Pulishing Company, Amsterdam, 1964, 653 – 673 http://nobelprize.org/nobel_prizes/chemistry/laureates/1962/perutz-lecture.pdf (10.10.06)
20. http://www.ks.uiuc.edu/Research/newbr/br_fig.html (10.10.06)
21. B. Alberts, D. Bray, J. Lewis, M. Raff, K. Roberts, J. D. Watson. Molecular Biology of the Cell, Garland Publishing, Inc. New York, 2.Edition, 1983
22. D. J. Aidley, P. Stanfield, *Ion Channels – Molecules in Action*, Cambridge University Press, Cambridge, UK, 1996
23. R. H. Ashley (Editor), *Ion Channels – a practical approach*, Oxford University Press, Oxford, USA, 1995
24. http://genomebiology.com/2003/4/3/207/figure/F1?highres=y (10.10.06)
25. R. G. Walker, A. T. Willingham, Ch. S. Zuker, *Science* **287**, 2229 – 2234 (2000)
26. http://www.cardiff.ac.uk/biosi/staff/jacob/teaching/ionchan/calcium_channel_structure.jpg (10.10.06)
27. P. A. Tipler, *Physik*, Spektrum Akademischer Verlag, Heidelberg, Germany, 2004
28. Schoen, P. Fromherz. *Appl. Phys. L.*, **87**, 193901, (2005)
29. M. H. Ulbrich, P. Fromherz. *Appl. Phys. A*, **81**, 887 – 891, (2005)
30. Tsumura, H. Koezuka, T. Ando. *Appl. Phys. Lett.* **49**, 1210 – 1212 (1986)
31. B. Singh, N. S. Sariciftci. *Annu. Rev. Mater. Res.,* **36**, 199 – 230, (2006)
32. P. Fromherz, A. Offenhausser, T. Vetter, and J. Weis. *Science* **252**, 1290 – 1293, (1991)
33. S. M. Sze, *Physics of Semiconductor Devices*, J.Wiley, New York, USA, 1981
34. F. L. Graham, J. Smiley, W. C. Russel, R. Nairn. *J. Gen. Virol.* **36**, 59 – 72, 1977
35. http://www.dow.com/PublishedLiterature/dh_003d/09002f138003dca8.pdf?filepath=cyclotene/pdfs/noreg/618-00219.pdf&fromPage=GetDoc (10.10.06)
36. Y. Kato, S. Iba, R. Teramoto, T Sekitani, T. Someya. *Appl. Phys. Lett.*, **84**, 3789 – 3791 (2004)
37. F-Ch. Chen, Ch-W. Chu, J. He, Y. Yang. *Appl. Phys. Lett.*, **85**, 3295 – 3297 (2004)
38. L. Wang, J. Yoshida, N. Ogata, S. Sasaki, and T. Kajiyama, *Chem. Mater.* **13**, 1273 (2001).
39. G. Zhang, L. Wang, J. Yoshida, and N. Ogata, *Proc. SPIE* **4580**, 337 (2001).

40. O.Mellbring, S. Kihlman Oiseth, A. Krozer, J. Laussmaa, T. Hjertberg. *Macromolecules*, **34**, 7496 – 7503 (2001)
41. E. Mizuno, M. Taniguchi, T. Kawai. *Applied Physics Letters,* **86**, 143513 (2005)
42. http://www.ncpri.ro/pullulan/en/My_Homepage_Files/Download/catalog_pull.pdf#search=%22pullulan%22 (25-09-06)
43. Dow Corning: http://www.dowcorning.com/applications/search/default.aspx?R=131EN,(10.10.06)
44. Th. Peterbauer, J. Heitz, M. Olbrich, St. Hering. *Lab on a Chip*, **6**, 857 – 863 (2006)
45. S. Bacchetti, F. L. Graham, *Proc Natl Acad Sci U S A*, **74**, 1590–1594 (1977)
46. http://www.microscopyu.com/articles/livecellimaging/fpintro.html, (24.10.06)
47. W. C. Heiser, Gene Delivery to Mammalian Cells Vol. 2: Viral Gene Transfer Techniques, Humana Press, 2004
48. http://www.fermentas.com/catalog/transfection/exgeninvitro.htm
49. http://cp.literature.agilent.com/litweb/pdf/5950-3000.pdf (10.10.06)
50. http://www1.qiagen.com/literature/qiagennews/0399/993infl.pdf
51. T. B. Singh, N. Marjanovic, G. J. Matt, N. S. Sariciftci, R. Schwödiauer and S. Bauer, *Appl. Phys. Lett.*, **85**, 5409 (2004
52. M. J. Panzer, Chr. R. Newman, C. D. Frisbie, *Appl. Phys. Lett.* **86**, 103503 (2005)
53. M. Halik, H. Klauk, Ute Zschieschang, G. Schmid, Chr. Dehm, M. Schütz, St. Maisch, F. Effenberger, M. Brunnbauer, F. Stellacci, *Nature*, 431, 963 – 966 (2004)

7. List of Figures

Figure 1: Interaction with the computer – now and in future? [8] 1
Figure 2: Iono-electronic interfacing by direct polarization (as in [14]) 3
Figure 3: Iono-electronic interfacing by indirect polarization via TEP (as in [14]) 4
Figure 4: Equivalent circuit for Point Contact Model (taken from [14]) 5
Figure 5: Equivalent circuit for Area Contact Model (taken from [14]) 5
Figure 6: The Cell (taken from [17]) 8
Figure 7: Lipid bilayer membrane (taken from [18]) 8
Figure 8: Phospholipids PC, PE, PS, SPHM 9
Figure 9: Use of transmembrane Proteins: transport, connections, receptor and enzymatic catalysis (taken from [16]) 10
Figure 10: Transport with the help of vesicles (taken from [16]) 10
Figure 11: X-Ray crystallographic structure analysis of transmembrane protein Bacteriorhodopsin (taken from [20]) 11
Figure 12: Possibilities for transmembrane transport (taken from [21]) 12
Figure 13: Voltage gated sodium channel (taken from [24]) 13
Figure 14: Pressure sensitive ion channels enable to hear (taken from [16]) 14
Figure 15: Voltage gated calcium channel (taken from [26]) 15
Figure 16: The capacitor 16
Figure 17: Common organic dielectrics: Polymethamethacrylat (PMMA), Polyimide (PI), Polytetraflourethylene (PTFE), Polyvinylalcohol (PVA), Polyethylene (PE) 17
Figure 18: Equivalent curcuit for LCR measurement (taken from [49]) 18
Figure 19: Angle θ in Impedance measurement 18
Figure 20: Doping mechanism and related applications (taken from [13]) 19
Figure 21: Used semiconductor materials: 20
Figure 22: MOSFET structure with p type semiconductor substrate (as in [33]) 20
Figure 23: a-Si:H thin film transistor (as in [33]) 21
Figure 24: Schematic Device structures (taken from [31] 21
Figure 25: Working principle of OFET with respect to applied gate voltage V_G (taken from [31]) 22
Figure 26: BCB monomer 25
Figure 27: BCB crosslinking reaction 25
Figure 28: Thermally cross linked BCB 26

Figure 29: Thermally cured polyimide 26
Figure 30: Crosslinked Polyvinylphenol 27
Figure 31: PMMA 27
Figure 32: CyEPl 28
Figure 33: Polystyrene 28
Figure 34: Polyethyleneoxide 29
Figure 35: Fura-2AM molecule 31
Figure 36: Ion channel activation experiment 32
Figure 37:Lipid-mediated transfection in mammalian cells (taken from [46]) 33
Figure 38: Successfully transfected HEK293 cells (taken from [48]) 35
Figure 39: Inverted microscope Axiovert 135 by Zeiss 35
Figure 40: MIM-Device 36
Figure 41: A typical microscopic image of HEK293 cells on glass slides 39
Figure 42: Cell clustering on top of untreated BCB 40
Figure 43: Slightly adhering cell cluster on treated BCB glass cover slide 40
Figure 44: HEK293 cells on untreated polyimide 41
Figure 45: Cells on NaOCl treated polyimide with semitransparent Cr/Au electrode (dark area) 41
Figure 46: HEK293 cells on untreated PVP_{xl} 42
Figure 47: HEK293 cells on NaClO treated PVP_{xl} 42
Figure 48: HEK293 on untreated PMMA 43
Figure 49: HEK293 on NaClO treated PMMA, day 3 after seeding 43
Figure 50: Maybe contaminated HEK29 cell culture on DNA-CTMA 44
Figure 51: Regular structures in DNA-CTMA based HEK293 cell culure 44
Figure 52: floating HEK293 cell clusters on CyEPl 45
Figure 53: Cracks on PS surface 45
Figure 54: HEK293 cell clusters on Sylgard® elastomer 46
Figure 55: HEK293 cell cultured on Pentacene 46
Figure 56: Detached Pentacene film on glass 47
Figure 57: HEK cell cluster floating above P3HT 47
Figure 58: HEK cell clusters on C_{60} 48
Figure 59: HEK cells on ZnPc 48
Figure 60: Transfection with Transfectin™: successfully transfected (right-hand side) cells with low yield but cells stay attached to the surface (left-hand side) 49

Figure 61: Transfection with Superfect™: successfully transfected (right-hand side) cells which detach from the surface and form clusters (left-hand side) 50
Figure 62: Transfection with ExGen500™: successfully transfected (right-hand side) cells which detach from the surface and form clusters (left-hand side) 50
Figure 63: Transfection with Lipofectamin™: successfully transfected (right-hand side) cells which detach from the surface and form clusters (left-hand side) 50
Figure 64: Electrode under direkt light (left) and under fluourescence light 51
Figure 65: Impedance vs. frequency measurement for sample with and without cells 52
Figure 66: Capacitance change under the influence of cells adhering to the dielectric surface 54
Figure 67: Transfer characteristic of top gate C_{60}/PI OFET 55
Figure 68: Output characteristics of top gate P3HT/PEO:$LiClO_4$ OFET 56
Figure 69: Transfer characteristic of top gate P3HT/PEO:$LiClO_4$ OFET 56

8. Appendix

8.1. Appendix A – Dulbecco's Modified Eagle Medium (GIBCO)

Inorganic Salts	**[mg/l]**
$CaCl_2.2H_2O$	264.0
$Fe(NO_3).9H_2O$	0.1
KCl	400.0
$MgSO_4.7H_2O$	200.0
NaCl	6400.0
$NaHCO_3$	3700.0
NaH_2PO_4	141.0

Vitamins	**[mg/l]**
D-Ca Pantothenate	4.0
Cholinchloride	4.0
Folacid	4.0
I-inositole	7.2
Nicotine amid	4.0
Pyridoxale HCl	4.0
Riboflavine	0.4
Thiamine HCl	4.0

Amino acids	**[mg/l]**
L-Arginine . HCl	84.0
L-Cysteine	48.0
L-Glutamine	580.0
Glycine	30.0
L-Histidine $HCl.H_2O$	42.0
L-Isoleucine	105.0
L-Leucine	105.0
L-Lysine.HCl	146.0
L-Methionine	30.0
L-Phenylalanine	66.0
L-Serine	42.0
L-Threonine	95.0
L-Thrptophan	16.0
L-Tryosine	72.0
L-Valin	94.0

Other Components	**[mg/l]**
D-Glucose	4500.0
Na-Pyruvate	110.0
Phenolred	15.0

The following supplements were added to the per 500 ml media:

10 % Fetal Calf Serum (FCS)

5 ml 100x L-Glutamine

10 ml 500x Penicillin/Streptomycin:

Penicillin (50000 IU/ml)

Streptomycin (5 mg/ml)

8.2. Appendix B: Transfection Protocols

Note: All specifications in the protocols are for one 3.5 cm Petri dish.

8.2.1. Transfection Protocol for Transfectin™ Lipid Reagent by *BIO-RAD*

1. Put 200 µl Dulbecco's MEM (without Fetal Calf Serum) in two Eppendorf tubes.
2. Pipet 1.5 µg DNA in one of the tubes.
3. Pipet 4 µl Transfectin™ Lipid Reagent into the other tube and mix it.
4. Transfer content of Tube 1 into tube 2 and gently mix it.
5. Incubate the mixture for 20 minutes at room temperature (RT).
6. Add mixture dropwise to cells in the Petri dish and gently rock the plate back and forth and from side to side to achieve even distribution of the complexes.
7. Incubate at 37 °C for 4 hours.
8. Change medium (DMEM + FCS).

8.2.2. Transfection Protocol for Superfect™ by *Quiagen*

1. Put 140 µl Dulbecco's MEM (without FCS) in two Eppendorf tubes.
2. Add 1.5 µg DNA to one of the tubes.
3. Add 7 µl Superfect™ Transfection Reagent to the other tube and mix it.
4. Transfer content of tube 1 to tube 2 and mix gently.
5. Incubate the mixture for 10 minutes at RT.
6. In the mean time: remove old media from Petri dish and add new DMEM + FCS
7. Add mixture dropwise to cells in the Petri dish and gently rock the plate back and forth and from side to side to achieve even distribution of the complexes.
8. Incubate at 37 °C for 2 hours.
9. Change medium (DMEM + FCS).

8.2.3. Transfection Protocol for ExGEN™ by *Fermentas*

1. Put 100 µl of 150 mM NaCl in an Eppendorf tube.
2. Add 1.5 µg DNA to the tube.
3. Add 3.3 µl ExGEN500™ to the tube

4. Immediately vortex the solution for 10 seconds.
5. Incubate the mixture for 10 minutes at RT.
6. Add mixture dropwise to cells in the Petri dish and gently rock the plate back and forth and from side to side to achieve even distribution of the complexes.
7. Incubate at 37 °C for 4 hours
8. Change medium (DMEM + FCS)

8.2.4. Transfection Protocol for Lipofectamin™ by *Invitrogen*

1. Put 100 µl FCS free Serum (Dulbecco's MEM in two Eppendorf tubes
2. Add 10 µl Lipofectamin™ Transfection Reagent to one of the tubes and incubated at RT for five minutes
3. Add 1 µg of DNA to the other tube.
4. Add tube 2 to tube 1 after 5 minutes and incubated at RT for 20 minutes.
5. Add mixture dropwise to cells in the Petri dish and gently rock the plate back and forth and from side to side to achieve even distribution of the complexes.
6. Incubate at 37° for four hours.
7. Change medium (DMEM + FCS).

8.3. Appendix C: Used equipment

- Evaporation machine UNIVEX350 (Leybold)
- Evaporation Control AS 053 (Leybold)
- Evaportaion Control IL820 (Intellemetrics)
- Glove box system MB 150 B-G/ MB 200 B (MBraun)
- Spin coater Model P6700 (Specialty Coating Systems)
- Eclipse TE200 microscope (Nikon)
- Axiovert 135 microscope (Zeiss)
- Monochromator Polychrome V (Till Photonics)
- 2 Channel (high power / medium power) source monitor unit E5273A (AGILENT Technologies)
- HP4284A Precision LCR meter (Hewlett Packard)
- Oven (Elektron Wärme Aachen) with JUMO process controller